Russian Chemical Reviews **76** (12) 1123 – 1137 (2007) © 2007 Russian Academy of Sciences and Turpion Ltd

DOI 10.1070/RC2007v076n12ABEH003745

Competitive cryochemical reactions of transition metal atoms, clusters and nanosized particles

T I Shabatina, J Mascetti, J S Ogden, G B Sergeev

Contents

I.	Introduction	1123
II.	Size effects in reactions of atoms and small clusters of transition metals (Sc, Ti, Cr, Fe, Co, Ni, Cu) with organic and inorganic molecules in inert matrices at low temperatures	1124
III.	Formation of metal nanoparticles in active matrices	1126
IV.	Thermal transformations of metastable complexes of lanthanide atoms and clusters	1128
V.	Competitive reactions of silver and gold particles of different sizes and shapes with model reagents	1131
VI.	Conclusion	1134

Abstract. Specific features of cryochemical reactions of transition metal atoms, small clusters, complexes and nanoparticles are considered. New phenomena that arise in nano- and subnanoscale systems at low temperatures are analysed. It is shown that the competition between self-assembly processes of metal atoms and reactions of metal aggregates of different size with organic and inorganic reagents determines the chemical nature and properties of the intermediate and final products. Special attention is paid to the analysis of size effects caused by the dependence of the reactivity of metal clusters and nanoparticles on the number of constituent atoms. Prospects for the use of competitive cryochemical reactions are discussed. The bibliography includes 185 references.

I. Introduction

Recent progress in cryochemistry was largely associated with the development of methods for synthesis and stabilisation of atoms, small clusters and nanoparticles incorporating from just a few metal atoms to hundreds and thousands.[1–5] At present, studies of these systems form the basis of a new direction of chemistry, namely, cryonanochemistry. In cryonanochemistry, attention is focused on the size effects associated with the dependence of the reactivity of clusters and nanoparticles on the number of constituting atoms.[1] Atoms and clusters that emerge in the thermal evaporation of metals in vacuum are much more reactive than bulk metals.[5] At low temperatures, these high-energy and extremely reactive particles undergo consecutive and competitive chemical reactions with different organic and inorganic molecules. Low-temperature covalent and non-covalent interactions lead to the formation of new chemical compounds of metals in the zero or lower oxidation states and to the stabilisation of unstable structures and labile coordinatively unsaturated complexes, radicals and unusual molecules. Such systems are of interest for coordination chemistry, chemistry of clusters and organometallic compounds, atmosphere and space chemistry. They may also be used in the development of new metal-containing nanomaterials and in the elaboration of new nanotechnologies.

This review analyses the experimental and theoretical data on competitive cryochemical reactions of metal atoms and small clusters in condensed media, namely, in solid matrices of inert gases (in the presence of one or two active reagents) and in low-temperature co-condensates containing reactive components, for the metals of the first, second and third transition rows. Special sections are devoted to thermal transformations of metastable mono- and polynuclear lanthanide complexes and to chemical reactions of silver and gold atoms, clusters and nanoparticles as the systems most promising for nanochemical and nanocatalytic applications. Attention is focused on the kinetic analysis of competitive chemical reactions that involve metal particles of different sizes and shapes with different ligands. Processes of formation and stabilisation of nanoparticles in low-temperature matrices and co-condensates are considered; mechanisms of their reactions with certain organic and inorganic reagents are discussed and manifestations of size effects typical of reactions of these small-scale chemical entities are analysed. In this review, almost no attention is paid to the problems associated with the development of a new promising research direction, *viz*., spectroscopic studies of metal clusters and their reactions in solid hydrogen matrices and liquid helium nanodroplets as condensed quantum systems. This is explained by the fact that these problems are of their own, independent importance.

The authors of this review are united by long-term collaboration within the framework of INTAS projects. The material of this review was partly presented as the plenary lectures at the VIth International Conference on Low Temperature Chemistry (Chernogolovka, 2006).

T I Shabatina, G B Sergeev Department of Chemistry, M V Lomonosov Moscow State University, Leninskie Gory, 119992 Moscow, Russian Federation. Fax/tel. (7-495) 939 54 42, e-mail: tsh@kinet.chem.msu.ru (T I Shabatina), gbs@kinet.chem.msu.ru (G B Sergeev)
J Mascetti Université Bordeaux I, Institut des Sciences Moléculaires, CNRS, 33405 Talence Cedex, France. Fax (33-540) 00 84 02, tel. (33-540) 00 63 60, e-mail: j.mascetti@ism.u-bordeaux1.fr
J S Ogden Department of Chemistry, University of Southampton, Highfield, SO17 1BJ Southampton, UK. Fax (44-2380) 59 37 81, tel. (44-2380) 59 23 54, e-mail: js.ogden@soton.ac.uk

Received 6 August 2007
Uspekhi Khimii **76** (12) 1202 – 1217 (2007); translated by T Ya Safonova

II. Size effects in reactions of atoms and small clusters of transition metals (Sc, Ti, Cr, Fe, Co, Ni, Cu) with organic and inorganic molecules in inert matrices at low temperatures

Reactions of transition metal atoms and clusters with organic and inorganic molecules attract keen attention. Indeed, such processes model the reactions of molecules of various reagents with the active sites on the metal catalyst surface, which allows study of unusual chemical processes including the activation of small molecules such as carbon dioxide and nitrogen.[6–8] Coordination of CO_2 to metal sites is the key stage of its catalytic and electrochemical reduction.[9–11] The method of matrix spectroscopy makes it possible to identify intermediate products of various reactions and elucidate the mechanism of metal coordination with ligand molecules.

The reactions of atoms of the 1st transition series elements (Sc, Ti, Cr, Fe, Co, Ni, Cu) with carbon dioxide were studied systematically by matrix Fourier transform IR spectroscopy (FT IR) using isotopically labelled molecules $^{13}CO_2$ and $C^{18}O_2$.[12–15] The obtained results together with density functional theory calculations made it possible to determine the equilibrium parameters of formed complexes and elucidate the coordination type of a metal. It was shown that in a carbon dioxide matrix at 10 K, metal atoms of the first transition rows (Fe, Co, Ni and Cu) form 1 : 1 complexes with CO_2 molecules. In these complexes, the coordination of these molecules to metal atoms was of the 'side-on' ($\eta^2_{O,O}$) type for nickel, the 'end-on' ($\eta^2_{C,O}$) type for copper and the C type (η^1_C) for iron (Fig. 1). The energy of a bond formed by a nickel atom with CO_2 was 17.5 kcal mol^{-1}, which is comparable with the binding energies of this atom in its complexes with similar molecules, namely $Ni(C_2H_4)$, $Ni(C_2H_4)_2$ and NiCO.[16–20] On the other hand, atoms of elements situated in the beginning of this period (Ti, V and Cr) effectively inserted into C–O bonds of CO_2 molecules to form oxocarbonyl derivatives (O)M(CO)(CO_2). According to calculations, the insertion of a titanium atom into a C–O bond of the CO_2 molecule proceeded virtually without activation and the thermodynamic stability of a (O)Ti(CO) molecule substantially exceeded the stability of possible complexes Ti(CO_2) (Fig. 2). The interaction of a titanium atom with the second CO_2 molecule resulted in the formation of an even more stable (O)Ti(CO)(CO_2) complex [$D_e(CO_2)$ = 28 kcal mol^{-1}, D_e is the energy of ligand bonding] in which the CO_2 molecule turned out to be in the 'side-on' coordination with respect to the titanium atom and the fragments (O)Ti(CO) and Ti(CO_2) were located in perpendicular planes.

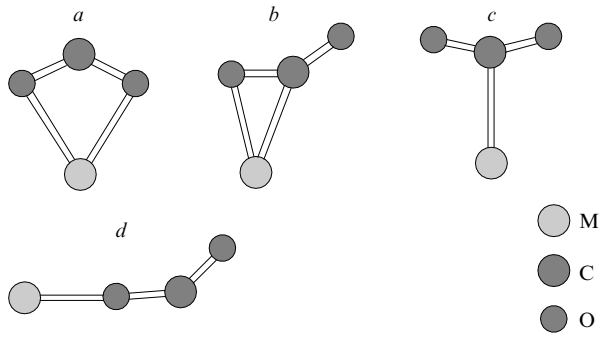


Figure 1. Types of complexes formed in the reaction of transition metals with CO_2.
Type: (*a*) $\eta^2_{O,O}$, (*b*) $\eta^2_{C,O}$, (*c*) η^1_C, (*d*) η^1_O.

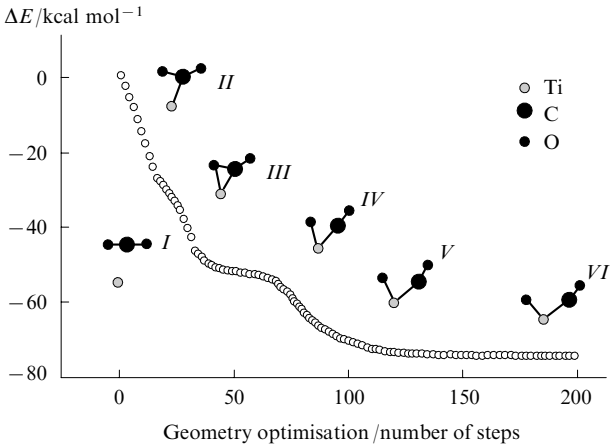


Figure 2. Possible structures of complexes formed in the titanium reaction with CO_2.[12]
(*I*–*VI*) are the types of structures corresponding to different steps of optimisation.

It was found[21] that excited titanium atoms insert into C–H bonds of ethylene molecules in argon matrices at 10 K upon irradiation of samples with light with a wavelength >400 nm. The TT IR method using isotopically labelled ethylene molecules $^{12}C_2H_4$, $^{13}C_2H_4$, C_2D_4, CH_2CD_2 and natural titanium isotopes revealed the formation of compounds containing Ti–C bonds, namely, titanacyclopropene $H_2Ti(C_2H_2)$ and vinyltitanium monohydride. The appearance of monoligand titanium π-complexes Ti(C_2H_4) was not confirmed experimentally, although model calculations carried out within the framework of the density functional theory (DFT) predicted the presence of strong bonding in this case. Titanium hydrides and carbonyls were obtained in the co-condensation of metal atoms with ligand molecules at superlow temperatures in inert matrices.[22–25]

In argon-diluted systems at low temperatures (10–30 K), virtually no interaction of atoms of the metal group under consideration with CO_2 was observed. The competitive interaction of nickel simultaneously with two ligands (N_2 and CO_2) in dilute argon matrices led to an unexpected result, the cooperative effect of co-ligands.[12] The binding of CO_2 molecules into a complex was substantially intensified when N_2 molecules were added to the argon matrix. The preliminary coordination of a nitrogen molecule into transient Ni(N_2) species induced the hybridisation of 4s and 3d orbitals of the nickel atom, which intensified the Ni → CO_2 charge transfer in a mixed-ligand complex Ni(CO_2)(N_2) as compared with a monoligand Ni(CO_2) complex. The obtained data are well described by a model 'electron donation L → M/back donation M → L' (the Chatt–Dewar–Duncanson model), which was used for the description of these systems.[26–28] A comparison of potential energy curves of these interactions have shown that the binding energy of a nickel atom with the CO_2 molecule is 17.5 kcal mol^{-1}, whereas the binding energy of a Ni(N_2) complex with the CO_2 molecule is almost twice as high, namely, 32 kcal mol^{-1}.

A reaction of copper with molecular nitrogen was studied in nitrogen and argon matrices by the FT IR and UV-Vis spectroscopic techniques.[29] In argon matrices with a constant ratio metal : matrix = 1 : 1000, the aggregation of metal atoms was determined by the nitrogen content. The Cu_2 : Cu ratio in a nitrogen matrix was larger than in an argon matrix and decreased upon dilution with argon. The co-condensation led to the formation of two complexes of copper dimers with the 'end-on' coordination of ligands, namely, mono- [$Cu_2(N_2)$]

and bisligand $[Cu_2(N_2)_2]$ complexes with binding energies of 7.9 and 12.8 kcal mol^{-1}, respectively.

No complexes were formed in argon-diluted systems with a ratio $N_2:Ar < 0.5$ that contained infinitesimal amounts of copper aggregates.[29] The interaction of copper atoms with nitrogen molecules started with the addition of a second ligand, CO, into the system. This was manifested by the formation of mixed complexes of copper atoms $Cu(N_2)CO$ for which the energies of ligand bonding [$D_e(Cu-CO) = 17.2$ and $D_e(Cu-N_2) = 7.5$ kcal mol^{-1}] were substantially higher as compared with the corresponding monoligand complexes, namely, 9.5 kcal mol^{-1} for Cu–CO and -0.1 kcal mol^{-1} for $Cu-N_2$. The strong polarisation of 4s orbitals in a dimer Cu_2 substantially weakened the σ-repulsion between the lone electron pair of a ligand and the $4s^13d^{10}$ electron shells of a copper atom in Cu_2L complexes. Thus, in the systems under consideration, dimeric nitrogen complexes $Cu_2(N_2)$ were preferentially formed.

Co-condensation of thermally evaporated copper atoms with carbon dioxide and an excess of argon afforded no reaction products. Co-condensation of copper vapour with an excess of carbon dioxide in the absence of matrix components led to the formation of 'end-on' monoligand complexes.[12] Density functional theory calculations using the 'Gaussian 03' computational package and the B3LYP functional were aimed at the comparison of reactivities of Cu atoms and Cu_2 dimers with respect to carbon dioxide and carbon disulfide.[30–32] The potential energy surface of the $Cu-CO_2$ system demonstrated a single minimum, which corresponded to the OCuCO insertion product with a potential barrier of 63 kcal mol^{-1} (Fig. 3). At the same time, a copper dimer Cu_2 in the singlet state underwent an activationless transformation into an 'end-on' complex $Cu_2(OCO)$ with the energy 2.1 kcal mol^{-1} lower than that of the starting reactants Cu_2 and CO_2. Based on the performed calculations, several insertion products into the C–O bond of carbon dioxide were proposed as other putative intermediate products (Fig. 4). As in the case of copper reaction with nitrogen molecules, the reactivity of a copper dimer turned out to be higher than that of a copper atom.

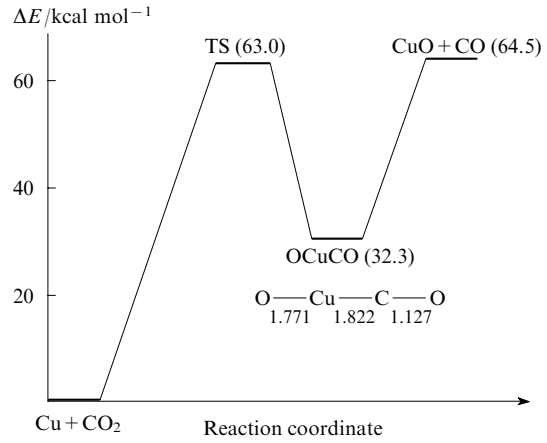


Figure 3. Potential energy variations in the $Cu + CO_2$ reaction and the structure of an intermediate product corresponding to the energy minimum (bond distances are shown in Å).[31]
TS is the transition state.

A series of $Fe_x(N_2)_y$ complexes were obtained in the reaction of mass-selected iron clusters with an excess of molecular nitrogen.[33] An IR spectroscopic study coupled with the Fourier analysis using isotopically labelled ligand molecules and the results of DFT simulations have shown 'end-on' $Fe(N_2)_5$ complexes to be the main reaction products of iron atoms with nitrogen molecules. Furthermore, cluster complexes $Fe_2(N_2)_x$ and $Fe_3(N_2)_x$ were observed. The early formation of $Fe_2(N_2)_x$ complexes ($x = 1-5$) in argon matrices was revealed by UV-Vis and IR spectroscopic techniques.[34] As in the case of copper, the ratio between the matrix-stabilised metal atoms and clusters $Fe:Fe_x$ was determined by the content of additionally introduced nitrogen. The maximum content of Fe_2 dimers was observed for the 0.05% nitrogen concentration in the argon matrix. For the higher nitrogen concentrations, iron dimers efficiently reacted with nitrogen

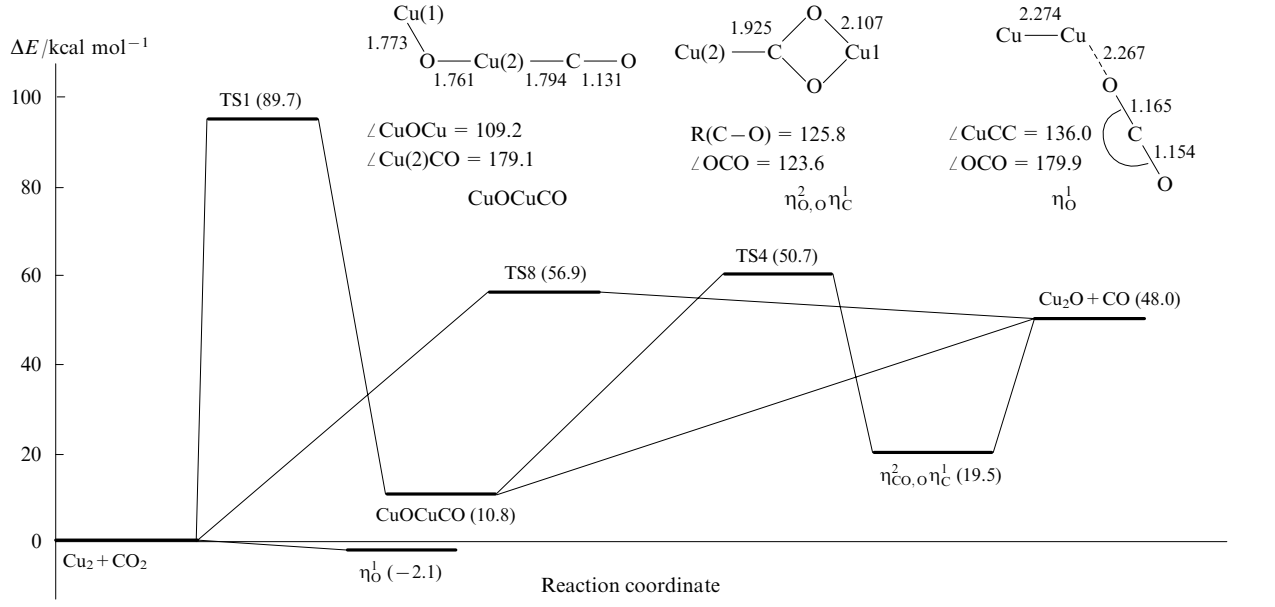


Figure 4. Potential energy variations in the reaction of a copper dimer Cu_2 (singlet state) with CO_2 and the structure of intermediate products corresponding to the energy minima (bond distances are shown in Å, angles are shown in degrees).[31,32]

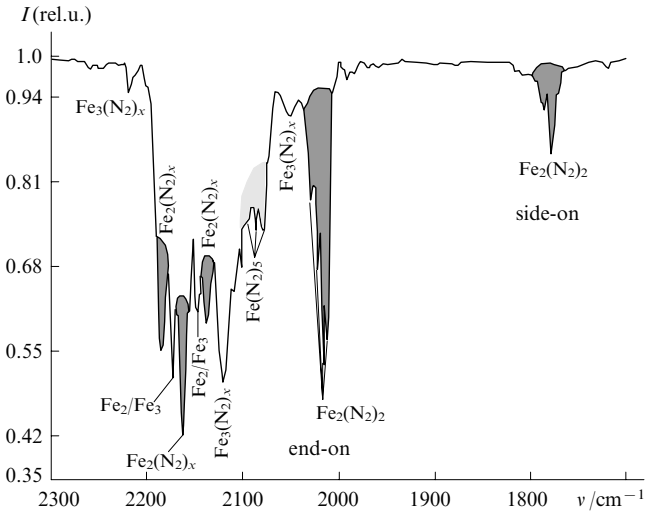


Figure 5. IR spectra of co-condensates of vapour of heat-evaporated iron and molecular nitrogen (T = 12 K, Fe : N_2 = 1 : 1000).[34]
Complex $Fe_2(N_2)_2$ exists in two forms, namely, 'end-on' and 'side-on'.

molecules to form diverse complexes with different coordination types (Fig. 5).

Co-condensation of nitrogen with certain metallocenes $M(Cp)_2$ ($Cp = \eta^5$-C_5H_5; M = Fe, Co, Ni, Mn, V) at 12–20 K afforded mixed-ligand complexes in which a nitrogen molecule was coordinated to a metal atom.[35–37] The reaction of iron porphyrin complexes with NO produced nitrosyl adducts of porphyrins that may be considered as a heme model.[38]

Co-condensates of transition metal vapours and aromatic hydrocarbons represent very reactive systems that produced mono- and bisarene complexes of transition metals and clusters and their more intricate complexes.[39] The reactions of chromium atoms and small clusters with benzene in argon matrices at 12 K were studied by FT IR, UV-Vis and resonance Raman spectroscopic methods.[39] The following chromium compounds were identified: $Cr(C_6H_6)$, $Cr(C_6H_6)_2$, Cr_2, $Cr_2(C_6H_6)$, $Cr_2(C_6H_6)_2$ and $Cr_3(C_6H_6)$. The use of selective photoexcitation of certain species allowed the authors to carry out a series of competitive chemical reactions of chromium atoms and dimers and their complexes

$$Cr + C_6H_6 \longrightarrow Cr(C_6H_6),$$

$$Cr + 2C_6H_6 \longrightarrow Cr(C_6H_6)_2,$$

$$2Cr \longrightarrow Cr_2,$$

$$Cr_2 + C_6H_6 \longrightarrow Cr_2(C_6H_6),$$

$$Cr_2 + 2C_6H_6 \longrightarrow Cr_2(C_6H_6)_2,$$

$$Cr_2 + Cr(C_6H_6) \longrightarrow Cr_3(C_6H_6),$$

$$Cr_2(C_6H_6) + C_6H_6 \longrightarrow 2Cr(C_6H_6),$$

$$Cr_2(C_6H_6)_2 \longrightarrow 2Cr(C_6H_6),$$

$$Cr_2(C_6H_6)_2 + 2C_6H_6 \longrightarrow 2Cr(C_6H_6)_2,$$

$$Cr_3(C_6H_6) + (5-x)C_6H_6 \longrightarrow xCr(C_6H_6) + (3-x)Cr(C_6H_6)_2.$$

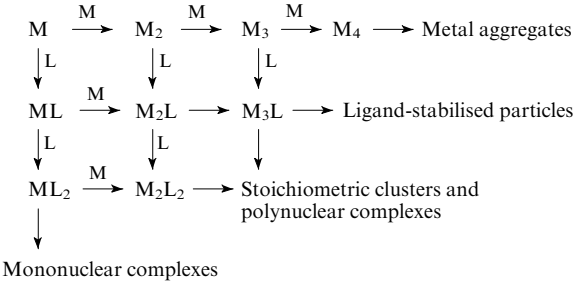
Exothermic reactions at low and ultralow temperatures (1.3–30 K) can also occur in the space on cosmic dust particles under the action of radiation.[40–47] The reactions of transition metals with polycyclic aromatic hydrocarbons are of undeniable interest for astrochemistry and astrophysics. It was assumed that such reaction products might be a source of certain unidentified radiation types observed in the interplanetary space.[48]

The possibility of these reactions was demonstrated by the FT IR spectroscopy in reactions of iron with pyrene and coronene in argon matrices at 4–10 K as an example.[49] It was found that pyrene forms unstable complexes with iron atoms, whereas coronene preferentially reacts with Fe_2 dimers to form mono- and bisligand complexes $Fe_2(C_{24}H_{12})_n$, where n = 1 or 2. These complexes were thermally stable up to 40 K and resistant to irradiation in the near UV and visible ranges (200–700 nm). Iron aggregates were easily formed in argon matrices with an increase in the metal concentration and exhibited the higher electron affinity (0.9 eV for Fe_2) as compared with an iron atom (0.15 eV); this explains the higher stability of their complexes. It is interesting that Fe_2 and Fe_3 clusters readily formed complexes with nitrogen molecules in binary Fe–N_2 systems, whereas no coronene complexes were detected in ternary Fe–coronene–N_2 co-condensates. This can serve as an indirect confirmation of the fact that coronene preferentially reacts with iron dimers. It is noteworthy that no coronene complexes were observed for nickel and titanium that do not form any aggregates under similar conditions.

III. Formation of metal nanoparticles in active matrices

The interaction of metal atoms with active ligand molecules in low-temperature co-condensates can be described as a sequence of competitive processes of aggregation of metal atoms and reactions of metal aggregates containing different numbers of nuclei with ligand molecules (Scheme 1).

Scheme 1



M is metal, L is ligand

The active-matrix molecules can play the role of ligands and form donor–acceptor or charge-transfer complexes with atoms and clusters. Depending on the temperature of the system and the concentrations of metal atoms and clusters, this may lead to the formation of mono- or polynuclear complexes and of nano- or subnanosized metal particles solvated with matrix molecules. Silver and copper feature the formation of different-sized clusters and nanoparticles in which a metal formally exists in the zero-valent state. Studying particles of different sizes makes it possible to follow the formation of the electronic and crystal structures of metals.

Silver and copper clusters and nanoparticles are easily formed at low temperature by the condensation of their vapours with the excess of an inert component,[50] thermo- and photo-aggregation of atoms[51] and by mass-spectral selection of clusters followed by their condensation in inert matrices.[2] Nanoparticles can be stabilised at room temperature provided the metal vapour is co-condensed with certain organic substances that are capable of specific non-covalent interactions and can form donor–acceptor complexes with transition metal atoms, clusters and nanoparticles.[52]

Metal particles measuring up to 10 nm were synthesised by low-temperature co-condensation of vapour of silver, copper, gold and other transition metals with acetone, ethanol, tol-

uene, trimethylamine, dimethylformamide, dimethyl sulfoxide and other compounds.[5] Heating of the co-condensate to room temperature afforded colloid solutions of nanoparticles with different stability that could be sputtered on different surfaces to form film coatings of various thickness.[52, 53]

Acrylic acid (AA), methyl acrylate (MA) and dimethylaminomethyl acrylate were also used for the stabilisation of silver nanoparticles.[54, 55] Low-temperature co-condensation of the metal vapour with MA followed by heating of the system to room temperature afforded stable silver organosols with 15 nm particles. Co-condensation with lead vapour produced bimetallic particles measuring < 5 nm. The transition from binary Ag/MA and Pb/MA systems to the ternary Ag/Pb/MA system was accompanied by non-additive changes in the properties. Polymerisation of MA was inhibited by lead and initiated by silver and the competition of these processes led to the formation of smaller bimetallic particles.[54] Co-condensation of silver vapour with 2-methylaminoethyl methacrylate afforded silver particles with diameters of 15–20 nm and their aggregates. Such cryochemical methods made it possible to synthesise silver particles dispersed in water, acetone and toluene, which were stabilised in the presence of poly(2-methylaminoethyl methacrylate).[55]

A method of stabilisation of copper nanoparticles in polyethylene was developed.[56] According to EXAFS and electron microscope studies, the average size of stabilised particles (copper nanocrystals) was 17 nm. A highly dispersed phase was formed upon decomposition of copper diacetate.

Low-temperature co-condensation of vapour of silver and copper and of Cd, Pb, Sn, Mn, Sm, Zn with the *p*-xylylene monomer, which undergoes easy polymerisation even at 100–120 K, was used in the synthesis of nanosized metal particles encapsulated in polymeric films.[57–59] The particle size determined by the transmission electron microscopy was 3–8 nm. The resulting films exhibited sensor and chemoresistive properties with respect to water and ammonia vapour.[60, 61]

Copper nanoparticles incorporated into poly(*p*-xylylene) in the course of low-temperature co-condensation of components were observed to exhibit high catalytic activity with respect to isomerisation of chlorine-containing compounds.[62, 63] The activity of these particles was two orders of magnitude higher than that of highly dispersed copper supported on silica gel.

Cryoformation of nanosized silver and copper particles in mesogenic alkylcyanobiphenyl matrices was studied in detail.[64–68] In co-condensates of silver and copper vapour with alkylcyanobiphenyl molecules at 80–90 K, low-temperature complexes of metal atoms were revealed.[69, 70] IR spectra of co-condensates demonstrated two new bands in the range of stretching vibrations. The characteristic bands of the CN group were shifted by -150 and -200 cm^{-1}, which pointed to the formation of silver and copper π-complexes with the cyanobiphenyl fragments of the matrix molecules. Indeed, the electron density shift from the binding orbital and the partial population of the antibonding orbital of the ligand should lead to loosening of the multiple bond in the complex, *i.e.*, to a decrease in the vibration frequency of the corresponding bond in the π-complex. Spectra of Ag/5CB and Ag/5CB/$C_{10}H_{22}$ (5CB is 4-n-pentyl-4′-cyanobiphenyl) co-condensates also exhibited new bands in the range of 650–660 cm^{-1}, which were attributed to the metal–ligand vibrations in π-complexes. The formation of π-complexes was confirmed by quantum chemical calculations performed for 4-n-pentyl-4′-cyanobiphenyl and its central cyanobiphenyl fragment.[71, 72] The structure of this complex includes two cyanobiphenyl fragments antiparallel to one another and a silver atom sandwiched between the CN fragment of ligand *1* and the centre of a benzene ring of ligand *2* (Fig. 6). In the ground state, the complex may acquire two electronic configurations, namely, a

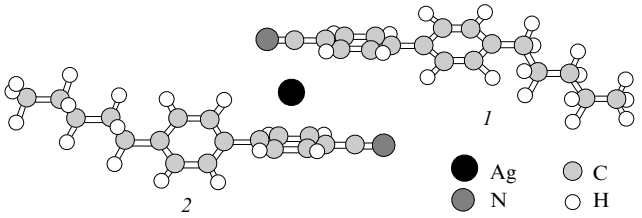


Figure 6. The structure of a bisligand silver complex with alkylcyanobiphenyl ligands $Ag(5CB)_2$;
(*1*, *2*) see text.

neutral complex $Ag(5CB)_2$ and a charge-transfer complex $Ag^+(5CB)_2^-$. For an interligand distance of 4.4 Å (the charge-transfer complex configuration), the calculated vibration frequency shifts of the C≡N bond in this complex as compared with this bond in the ligand molecule were -150 and -175 cm^{-1}, which were consistent with the experimentally observed values of -150 and -200 cm^{-1} for Ag/5CB films at 90 K.

EPR spectra of Ag/5CB samples contained a doublet of doublets (*A* and *B*, low-field and high-field spectrum components) with *g*-factors of 2.001, 2.003 and hyperfine coupling (HFC) constants of 48.5 and 55.7 mT, respectively (Fig. 7).[70] The analysis of literature data[73, 74] suggests that the appearance of components *A* and *B* in the EPR spectrum is the result of the formation of π-complexes of silver atoms (^{107}Ag and ^{109}Ag) with cyanobiphenyl molecules. A comparison of HFC constants of silver atoms in the obtained samples with those of atoms stabilised in an inert hydrocarbon matrix (63.22 and 72.75 mT for ^{107}Ag and ^{109}Ag, respectively) allowed assessment of the spin density on the Ag atom as 0.89. This value is typical of π-complexes with metal atoms and points to the partial donation of the electron density from occupied orbitals of a metal atom to the antibonding π*-molecular orbital of a ligand.

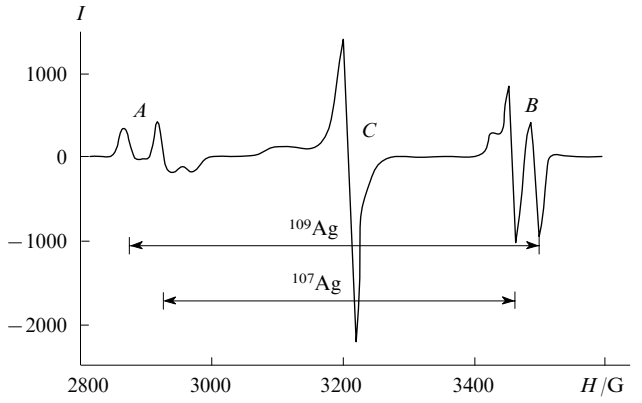


Figure 7. EPR spectrum of an Ag/5CB co-condensate at 80 K.[68]

In EPR spectra of Cu/5CB co-condensates, an anisotropic quartet signal of a cyanobiphenyl complex of a copper atom was detected ($J = 3/2$).[66, 75] Spin-resonance parameters of complexes were as follows: $g_{xx} = g_{yy} = 2.007$, $g_{zz} = 1.981$, $A_{iso} = 19$ mT; HFC on ^{63}Cu and ^{65}Cu isotopes were unresolved due to the close *g*-factors of their nuclei. The relatively low HFC constants for copper together with the highly anisotropic signal suggested that the highest occupied molecular orbital in a complex that contained a lone localised electron was of the hybrid nature and that the electron density

was shifted from a metal atom to ligand molecules. The spin density on the metal atom did not exceed 0.1.

The EPR spectra of co-condensates also revealed a central signal *C* (see Fig. 7) with a *g*-factor close to that of a free electron (2.003). The signal could be caused by the conducting electrons spin resonance (CESR) from a set of nanosized metal clusters and their complexes stabilised in the 5CB matrix. Similar signals were also observed for sufficiently concentrated silver and copper co-condensates with saturated hydrocarbons and inert gases.[76,77] This signal represented a superposition of several isotropic lines of Lorentzian shape. The *g*-factor and the widths of signal line depended on the size of metal particles due to the difference in the spin–lattice relaxation times (T_1). Taking into account the presence of experimental *g*-factor shifts, the average size of metal particles stabilised in cyanobiphenyl matrices at 90–120 K was assumed to be 1–2 nm. An increase in the Ag to 5CB ratio led to the domination of processes of silver aggregation in the system, which substantially decreased the yield of this complex. On heating of co-condensates from 90 to 150 K, the relative intensity of doublet lines of silver complexes (quartet lines for copper complexes) decreased and the relative intensity of the central component increased, which pointed to the thermal decomposition of metastable complexes and the increase in the concentration of nanosized metal clusters due to the spontaneous aggregation of metal atoms that emerge in the system.

Studies of electron absorption spectra for the Ag/5CB and Ag/5CB/decane systems confirmed the results obtained by IR and EPR spectroscopic techniques. UV-Vis spectra of Ag/5CB co-condensates at 80 K (Fig. 8, curve *1*) revealed a structured absorption band of a silver complex with a peak at 360 nm, which corresponded to light-yellow co-condensate films. Quantum chemical simulation of excited states of this complex pointed to the presence of several intense charge-transfer transitions metal–ligand and ligand–ligand in the range of 360–400 nm.[78] The absorption at 360 nm disappeared as the co-condensate film was annealed to 200–300 K. A broad band with the peak at 420 nm that appeared at these temperatures (see Fig. 8, curves *2*, *3*) was probably due to the absorption of surface plasmons of nanosized silver particles[79] formed as a result of aggregation of silver atoms and small clusters during the thermal decomposition of the complex. According to the data of transmission electron spectroscopy, depending on the phase state of the Ag/5CB system, two types of particles were formed, namely, globular with the average diameter of 15 nm and anisotropic rod-like particles ~200 nm long. The increase in the metal concentration and aggregation in an orientation-ordered mesophase favoured the formation of rod-like metal particles.[80,81]

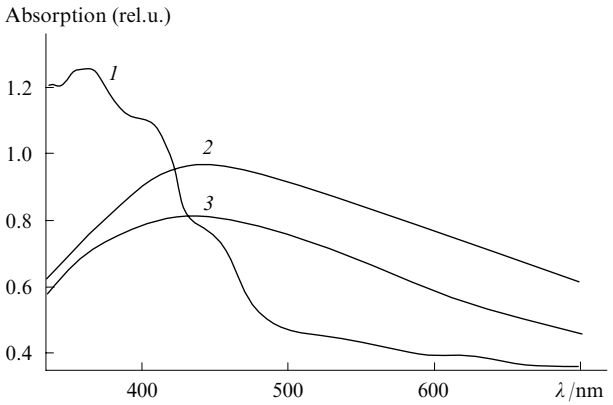


Figure 8. Optical spectra of silver co-condensates with 4-n-pentyl-4′-cyanobiphenyl at different temperatures.[69]
T/K: (*1*) 80, (*2*) 200, (*3*) 300.

Thus, metal complexes appear in the course of low-temperature co-condensation of metal vapour and reactive organic components containing functional complexing groups. Annealing of this system leads to the thermally induced decomposition of unstable complexes and the matrix-controlled aggregation of metal atoms and small clusters of different sizes and shapes. The chemical nature and properties of the resulting reaction products are determined by the competition between self-assembling processes and the reactions of different-sized metal aggregates with molecules of reagents added to the system.

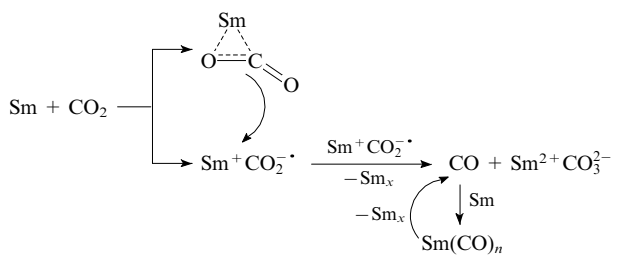
IV. Thermal transformations of metastable complexes of lanthanide atoms and clusters

As was shown above, cryochemical synthesis allows one to obtain new compounds and complexes for a series of d-metals in unusual oxidation states and with unusual coordination of ligand molecules. Competitive cryochemical reactions of lanthanide atoms with certain organic and inorganic ligands also lead to unusual products, where both the changes in the oxidation state and the formation of complexes between zero-valent lanthanides and CO, ethylene, tri(*tert*-butyl)benzene and its derivatives can be expected.[81–84]

The majority of reactions of lanthanide atoms lead to the changes in the metal oxidation state. Their reactions with oxygen were studied by the example of cerium, praseodymium, terbium and europium. Europium formed several oxides and peroxides with different compositions, namely, EuO_2, Eu_2O_4, Eu_2O_3, $EuO_2 \cdot Eu_2O_2$.[85] Cerium, praseodymium and terbium produced mixtures of oxides LnO and peroxides LnO_2.[86] The reaction of gadolinium with chlorine in argon matrices afforded $GdCl_3$. In the case of holmium, this reaction produced a mixture of comparable amounts of metal dichloride and trichloride and the monochloride HoCl; for ytterbium, a mixture of dichloride and trichloride was formed. Europium formed a mixture of dichloride and trichloride, where the former prevailed. No formation of europium monochloride was detected. All the products were identified by IR spectroscopy.[87] Under similar conditions, reactions of holmium and europium with bromine and iodine were carried out. It was shown that with bromine, both lanthanides produce di- and tribromides in comparable amounts. Their reaction with iodine also afforded di- and triiodides, where diiodide dominated for europium and triiodide prevailed for holmium. IR spectra of iodine co-condensates with holmium and europium also contained bands that could be assigned to polymeric iodides.[88]

The reaction of samarium with alkyl halides was studied under conditions of matrix isolation in the temperature range of 12–30 K.[89] IR spectroscopic data revealed the formation of methane in this reaction. Under conditions of matrix isolation, a reaction of samarium with CO_2 was studied.[89,90] Based on the IR and UV spectroscopic data, the reaction sequence shown in Scheme 2 was proposed.

Scheme 2



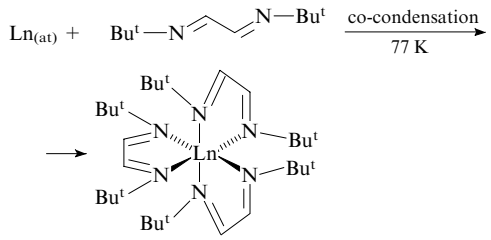
Straight lines mean that the corresponding reaction occurs at the condensation temperature (12 K); curved lines correspond to the reaction on heating (30 K)

The reactions of samarium with alcohols (ROH) were studied.[91–94] These reactions afforded the corresponding hydrocarbons RH and samarium alkoxides $Sm(OR)_x(OH)_{3-x}$. The reaction products contained insignificant amounts of doubled alkanes R–R, which pointed to the radical mechanism of this process. In the first stage, samarium atom was inserted into the C–O bond of an alcohol molecule to form RSmOH and trivalent samarium alkoxide $Sm(OR)_3$. For isopropyl alcohol, a cluster compound $Sm_5O(OR)_{13}$ could also be formed.[94] The composition of this compound was revealed by elemental analysis and NMR spectroscopy.

Cryocondensation of samarium with acetone followed by annealing of the co-condensate and hydrolysis led to a set of saturated and unsaturated hydrocarbons and alcohols, namely, $CH_3CH{=}CH_2$, C_3H_8, $(CH_3)_2CHCH(CH_3)_2$, $(CH_3)_2C{=}C(CH_3)_2$, $(CH_3)_2CHOH$ and samarium hydroxide.[95] A samarium cryocolloid produced in the co-condensation of samarium atoms with an unsaturated hydrocarbon reacted with acetone and the co-condensate was heated to its melting point. Co-condensation of metals with acetylacetone also produced samarium, holmium, erbium and disprosium acetylacetonates.[96] Furthermore, the co-condensation of samarium, acetylacetone and dimethyl sulfoxide afforded a samarium acetylacetonate adduct to dimethyl sulfoxide.[96]

Co-condensation of lanthanide atoms with substituted diazabutadiene $Bu^tN{=}CHCH{=}NBu^t$ (Bu^tDAB) led to the formation of a chelate complex containing three ligand molecules (Scheme 3).[97,98]

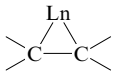
Scheme 3



Ln = Y, Nd, Sm, Eu, Gd, Ho, Yb.

The structure of the samarium complex was studied by X-ray diffraction analysis. It was shown that five-membered rings Sm–N–C–C–N–Sm are virtually planar, deviating by 0.051 Å from the plane. The C=N bond distance was 1.35(3) Å, which is much longer as compared with the free ligand [1.283(6) Å]. This may be due to the electron density transfer from a metal atom to the lowest unoccupied molecular orbitals (LUMO) of the ligand to form Ln^{2+} and Ln^{3+} ions. This is why it is more correct to represent the samarium complex and analogous compounds of the lanthanides as the complexes formed by trivalent metals with radical anions, *i.e.*, $[Ln^{3+}(Bu^tDAB^{-\bullet})_3]$. The analogous ytterbium compound $[Yb^{3+}(Bu^tDAB^{-\bullet})_3]$ had a magnetic moment of 5.9 μ_B in the solid state at room temperature and 2.4 μ_B at $T < 100$ K. A model was proposed according to which this compound exists in two forms, namely, as $[Yb^{3+}(Bu^tDAB^{-\bullet})_3]$ at temperatures above 100 K and $[Yb^{2+}(Bu^tDAB^{-\bullet})_2(Bu^tDAB)]$ at lower temperatures. The calculated magnetic moments of these species were 5.5 and 2.45 μ_B, respectively, which was consistent with the experimental data. Erbium, neodymium and samarium co-condensation with buta-1,3-diene produced analogues products, namely, $Ln(C_4H_6)_3$.[99] The introduction of dimethylbutadiene into this reaction resulted in the formation of complexes with the composition $Ln[(CH_3)_2C_4H_4]_2$. The magnetic susceptibility measurements have shown that in all the cases, the degree of oxidation of lanthanide atoms was 3+.

Co-condensation of samarium, erbium and ytterbium vapours with hydrocarbons containing double bonds, namely, ethylene, propylene and allene, led to the formation of products that afforded a mixture of saturated and unsaturated hydrocarbons from C_1 to C_6 upon hydrolysis. This suggests that the reaction mechanism is rather complex and involves the insertion of lanthanide atoms into the C–C bond to form a ring



or a chain Ln–C–C–Ln.[100]

Low-temperature reactions of ytterbium, erbium and samarium with terminal alkynes afforded products with absorptions in the range of 2020–2060 cm^{-1} (triple bond vibrations), namely, $(YbC_9H_{14})_n$, $(ErC_{12}H_{19})_n$ and $(SmC_{12}H_{19})_n$.[101] Co-condensation of samarium atoms with hexane gave rise to the evolution of hydrogen; hydrolysis of the co-condensate produced hex-1-yne and insignificant amounts of destruction products.[102] Experimental data suggest the following reaction sequence:

$$Sm + n\,R{-}CH_2{-}CH_3 \longrightarrow [R{-}C{\equiv}C{-}Sm{-}H\cdot 2\,H_2] \longrightarrow$$
$$\longrightarrow R{-}C{\equiv}C{-}Sm{-}H + 2\,H_2.$$

R = n-C_4H_9.

Co-condensation of samarium vapour with 1-bromopentane at 80 K afforded green films. On heating, a mixture of saturated and unsaturated hydrocarbons, namely, pentane, decane and pentene, was obtained. Results of EPR studies gave grounds for assuming the radical mechanism of this process.[103]

At present, several reactions of lanthanide atoms and clusters are known to involve no changes in oxidation state. It was assumed that for efficient complexation a lanthanide atom should acquire the $4f^{n-1}5d^16s^2$ configuration as a result of the transition of one f electron to the d shell.[102] The energy of excitation of an f electron to the d sublevel is of crucial importance for this process. Figure 9 illustrates the dependence of this energy on the degree of population of the f shell. The interaction of lanthanide atoms with CO molecules was studied for a series of metals, namely, Pr, Nd, Sm, Eu, Gd, Ho and Yb, in an argon matrix at 10–40 K using the electronic and IR spectroscopic methods.[104–106] In the majority of cases, carbonyls $Ln(CO)_x$ were formed (x = 1–6). Heating of the

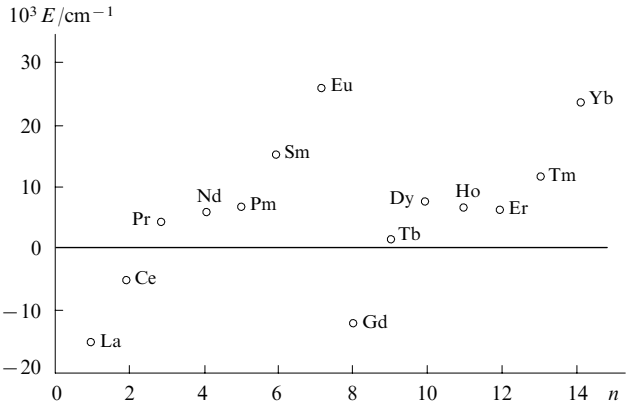


Figure 9. Calculated excitation energy $[f^ns^2] \rightarrow [f^{n-1}d^1s^2]$ as a function of the degree of population of the f orbital of a non-excited lanthanide atom.[82]

system to 15–40 K transformed the lower carbonyls to the higher, $Ln(CO)_6$. In a range >40 K, carbonyls of all metals underwent destruction, where the destruction temperature corresponded to the matrix melting point. The distinguishing feature of samarium and europium is that they did not form carbonyls at $x = 1-3$ for Sm and $x = 1, 3$ for Eu. It should be mentioned that the decomposition temperature of the higher samarium carbonyl (30 K) was lower as compared with the higher europium carbonyl (40 K), which is in conflict with their excitation energies (see Fig. 9). Gadolinium carbonyl that has a d electron in the ground state also proved to be unstable. The most stable carbonyls were formed by metals with the larger number of d-electrons, *e.g.*, by Cr, Mn, Fe, Co, Ni.

Reactions with ethylene were studied in detail for europium and samarium atoms and clusters in argon matrices and also for samarium co-condensates with ethylene.[89, 107] It was found that two complexes, $Ln(C_2H_4)$ and $Ln(C_2H_4)_2$, are formed. On gentle heating, the monoligand complex was transformed to the biligand complex. Taking into account the presence of free samarium atoms even in non-dilute ethylene, it can be assumed that the formation of a Ln·L complex and its subsequent transformation to Ln·2 L are limited by the rotational diffusion. The decomposition temperature of the higher europium complex (~60 K) exceeded that of the higher samarium complex (~40 K). The structure of the monoligand samarium complex with ethylene was studied.[107] It was assumed that this complex is stabilised due to weak direct interaction of half-occupied metal f orbitals with σ and π orbitals of their ligand.

Reactions of lanthanides with aromatic ligands, namely, 1,3,5-tri(*tert*-butyl)benzene (TTB), 2,4,6-tri(*tert*-butyl)pyridine (TTPy) and 2,4,6-tri(*tert*-butyl)phosphorine (TTP), were studied in their co-condensates in the temperature range of 80–373 K.[82, 83, 108, 109] The structure of a single crystal of the gadolinium TTB complex was determined by X-ray diffraction analysis. The molecules of the complex had a sandwich structure with a metal atom located between two benzene rings in the staggered conformation. The LUMO energy of heteroaromatic ligands is lower than the LUMO energy of benzene, which leads to the stronger interaction of ligands with the metal d orbitals. As a result, on going to analogous heteroaromatic complexes of lanthanides, the bond becomes stronger and the decomposition temperature increases (Table 1). The bond strength in lanthanide complexes with aromatic ligands increased with the decrease in the metal atom radius, the reduction of the energy of f electron excitation and the lowering of the LUMO energy of the ligand.[82, 109]

Samarium complexes with 4-n-pentyl-4′-cyanobiphenyl were detected in an argon matrix at 6–10 K and in Sm co-condensates with 5CB at 80–240 K.[110, 111] The formation of such complexes was revealed by the appearance of new absorption bands in the IR spectra, namely, a triplet band at 2170 cm^{-1} (complex *I*) and 2060 cm^{-1} (complex *II*) (Fig. 10). The bands were shifted to lower frequencies as compared with vibrations of the CN group of the ligand (2230 cm^{-1}). This made it possible to assign new bands to CN vibrations in π-complexes. Splitting of a band at 2170 cm^{-1} to three components can be associated with the stabilisation of different complex configurations in a low-temperature argon matrix and also with different local environment. The activation energy of the formation of complexes was close to zero, which confirmed their formation at 6–10 K. The first complex was formed at 6–10 K in a molar ratio Sm : 5CB : Ar = 1 : 33 : 10 000. At such dilution, the aggregation of metal atoms was absent, and the complex was formed from samarium atoms. The composition was determined by a modified method of multiple ratios in a series of experiments on the joint condensation of samarium and 5CB with a 100–1000-fold excess of decane. The stoichiometric composition was M·2 L for complex *I* and M·L for complex *II*. Bearing in mind the tendency of lanthanide atoms for the formation of bisligand sandwich complexes and the susceptibility of cyanobiphenyl molecules to dimerisation at low temperatures,[112] the second complex was also considered as a bisligand binuclear 2 M·2 L complex.

Table 1. Decomposition temperatures (K) of lanthanide complexes with different ligands.

Ln	Ground state	TTB	TTPy	TTP
La	d^1s^2	263	–	283
Ce	$f^1d^1s^2$	–	–	–
Pr	f^3s^2	318	–	–
Nd	f^4s^2	>373	–	–
Sm	f^6s^2	213	223	223
Eu	f^7s^2	190	225	–
Gd	$f^7s^2d^1s^2$	>373	–	–
Tb	f^9s^2	>373	–	–
Dy	$f^{10}s^2$	>373	–	–
Ho	$f^{11}s^2$	>373	–	>443
Er	$f^{12}s^2$	>373	–	–
Tm	$f^{13}s^2$	–	–	–
Yb	$f^{14}s^2$	–	–	–
Lu	$f^{14}d^1s^2$	>373	–	–

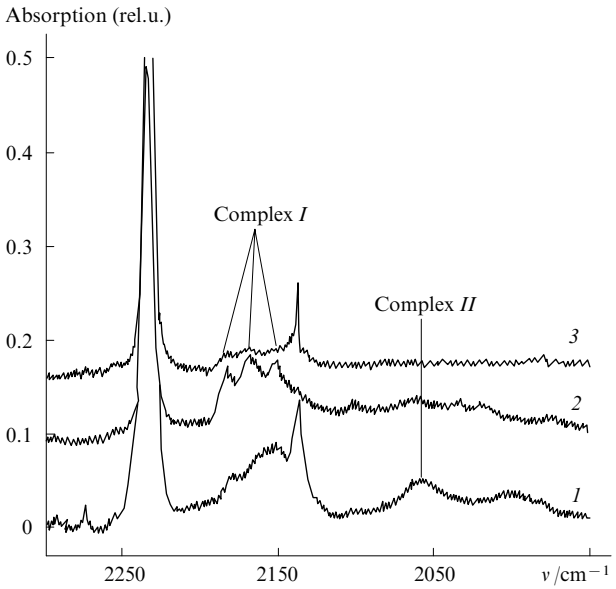


Figure 10. IR spectra of complexes Sm·5CB isolated in an argon matrix.[110]
(*1*) Molar ratio Sm : 5CB : Ar = 1 : 10 : 400, $T = 6.5$ K; (*2*) 1 : 24 : 5000, $T = 10.5$ K; (*3*) 1 : 33 : 10 000, $T = 10.5$ K.

In the temperature range of 80–95 K, samarium co-condensates with 4-n-pentyl-4′-cyanobiphenyl in a molar ratio M : L = 1 : 10 contained only the complex M·2 L.[113, 114] As the sample was heated to 210 K, the absorption band of the complex M·2 L disappeared and a band of the complex 2M·2 L emerged. Heating above 210 K led to the decomposition of both complexes. The complex M·2 L absorbed in the visible range at 400 nm, while the complex 2M·2 L absorbed at 420 nm. The UV spectrum of the Sm/5CB co-condensate contained an absorption band of the complex M·2 L at 400 nm at 95 K. As the temperature increased, a shoulder at 420 nm appeared, which corresponded to the complex 2 M·2 L. Electronic spectra of co-condensates demonstrated a broad long-wavelength absorption band with a peak at

$\sim$600 nm, which can be assigned to the absorption of metal nanoparticles. An increase in the length of the hydrocarbon substituent chain in the ligand molecule had no effect on the stability of complexes. On going from 5CB to its heteroaromatic analogue, 4-n-pentyl-4′-cyanophenylpyridine (5Py), the stability of complexes increased.[114] The IR spectrum of the co-condensate at liquid nitrogen temperature contained a single band at 2150 cm^{-1}, which corresponded to the complex $Sm \cdot 2(5Py)$. As the temperature increased to 230 K, a new band at 2100 cm^{-1} appeared ($Sm \cdot 5Py$). The thermal decomposition of complexes occurred above 230 K, *i.e.*, 20 K higher as compared with the Sm/5CB system. This can be associated with the stronger metal–ligand bonding in complexes $Sm \cdot 5Py$. On going from samarium to europium, the thermal stability of the complex $Ln(5CB)_2$ also increased.

Model calculations of structures of complexes were carried out in terms of the density functional theory with the B3LYP exchange-correlation potential using the NWCHEM programme.[115,116] Only the ligand part involved in the complexation was considered. The optimised structures had the form of sandwiches (Fig. 11). The most stable state was reached at multiplicity 10 for complex *I* and multiplicity 15 for complex *II*; the binding energies were 10.6 and 31.3 kcal mol^{-1}, respectively. Multiplicity substantially affected the values of a torsion angle between the benzene ring planes of one ligand (φ_1), an angle between benzene ring planes of two ligands (φ_2) and an angle formed by axes of ligands (φ_3). In the complexation, the stretching frequency of the cyanobiphenyl CN group in both complexes shifted to lower values, which was consistent with the experimental data.

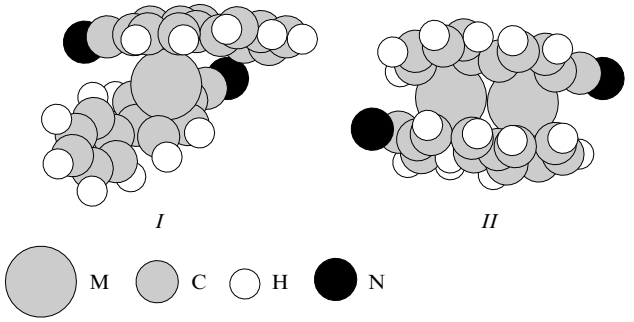


Figure 11. Optimised structures of complexes $M(CB)_2$ (*I*) and $M_2(CB)_2$ (*II*).[115]

The equilibrium structures and complexes formed by europium atoms and their dimers with non-substituted cyanophenylpyridyl ligands were simulated using quantum chemical methods.[117] For mononuclear complexes, the competition between two mechanisms of metal atom coordination was observed, namely, between the formation of sandwich π-complexes, which is caused by the interaction with π orbitals of the ligand, and the σ-coordination to the nitrogen atom of the pyridine ring. Sandwich structures of alkylcyanophenylpyridyl ligands were stabilised as a result of intermolecular N···H contacts between the nitrogen atom of the cyano group and the terminal hydrogen atom of the ethyl group. The higher thermal stability of the binuclear complex was demonstrated.

As the temperature of Sm/5CB and Sm/5Py co-condensates increased from 183 to 223 K, simultaneous decay of SmL_2 signals and growth of Sm_2L_2 signals were observed in the IR spectra (Fig. 12). This pointed to the transformation of mononuclear complexes ML_2 to binuclear complexes M_2L_2.[118,119] The following kinetic scheme, which includes the competition between processes of metal atom aggregation and their interaction with ligand molecules, was proposed:

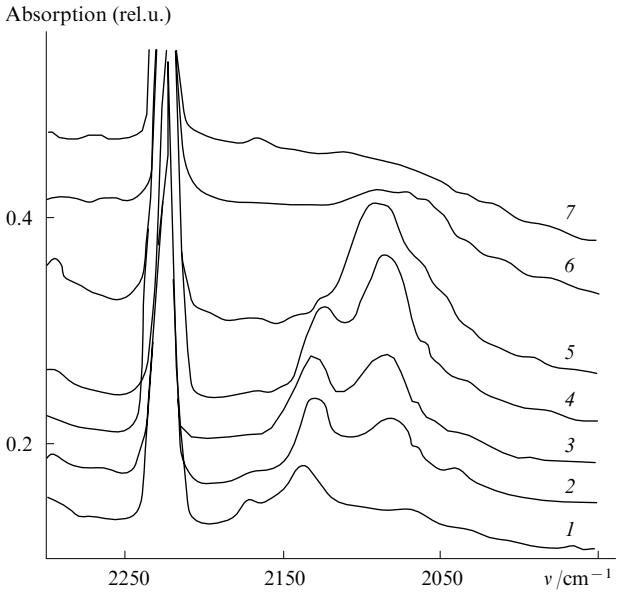


Figure 12. IR spectrum of a Sm/5CB co-condensate at different temperatures.[111]
T/K: (*1*) 8, (*2*) 163, (*3*) 183, (*4*) 203, (*5*) 223, (*6*) 243, (*7*) 273.

$$Sm + L_2 \longrightarrow SmL_2 \text{ (during condensation)}, \quad (1)$$

$$SmL_2 \longrightarrow Sm + L_2, \quad (2)$$

$$Sm + Sm \longrightarrow Sm_2, \quad (3)$$

$$Sm_2 + L_2 \longrightarrow Sm_2L_2, \quad (4)$$

$$Sm_2L_2 \longrightarrow Sm_2 + L_2, \quad (5)$$

$$Sm + Sm_x \longrightarrow Sm_{x+1} \ (x \geqslant 1). \quad (6)$$

The consumption of a complex ML_2 at this temperature did not reach zero but stopped at a certain degree of transformation, which is typical of multistep chemical reactions in the solid phase.[120] As the temperature increased, the degree of transformation increased. The effective activation energies were 17.5 and 18.5 kJ mol^{-1} for 5CB and 5Py, respectively. The results of experimental and theoretical studies [113–119] have demonstrated the importance of taking into account the competitive reactions of metal atoms and aggregates when analysing the thermal transformations of complexes in low-temperature co-condensates.

V. Competitive reactions of silver and gold particles of different sizes and shapes with model reagents

Studies of competitive chemical reactions of metal particles in different degrees of aggregation with model chemical reagents attracted special attention.[121,122]

Competitive reactions of silver and copper atoms and clusters, which were stabilised in a nanostructurised 4-n-pentyl-4′-cyanobiphenyl matrix, with carbon tetrachloride as a model reagent, were studied by EPR and UV-Vis spectroscopic techniques.[122–125] EPR spectra of ternary co-condensates of silver with carbon tetrachloride and 4-n-pentyl-4′-cyanobiphenyl, which contained CCl_4 in a concentration varying from 0 mol % to 10 mol % with respect to cyanobiphenyl, were studied at 80–300 K. For systems with $[CCl_4]:[5CB] \leqslant 0.03$, only doublet signals of π-complexes formed by silver atoms with cyanobiphenyl ligands $Ag(5CB)_2$

were observed. The addition of carbon tetrachloride to the system led to the formation of several paramagnetic products of competitive reactions of silver atoms and clusters with 5CB matrix molecules and added CCl_4. Heating–cooling cycling of samples and computer simulations of spectra corresponding to different temperatures and different component concentrations made it possible to reveal several paramagnetic species, namely, nanosized metal particles, a σ-complex of a silver atom with two ligands (5CB and CCl_4) and an adduct of trichloromethyl radical to silver chloride $AgCl-\dot{C}Cl_3$ (Ref. 125).

Annealing of co-condensates at 90–200 K changed relative intensities of signals under consideration. Figure 13 shows the temperature dependences of yields of paramagnetic products formed in the reactions of silver atoms and nanosized clusters with carbon tetrachloride and matrix (5CB) molecules for co-condensates with different ratios of reagents (Ag, CCl_4 and 5CB). In the temperature range of 90–120 K, the doublet signals of a π-complex formed by silver atoms with 5CB matrix molecules, which could be detected in systems with low CCl_4 concentrations, were observed to decay. This was caused by the thermal decomposition of the π-complex. Simultaneously, for samples with low carbon tetrachloride concentrations, an increase in the intensity of signals of silver nanoclusters was observed (see Fig. 13 *a*). At the same time, samples with higher CCl_4 concentrations demonstrated no increase in intensity of signals of silver nanoclusters (see Fig. 13 *b*).

These changes were attributed to the reactions of silver atoms, which emerge in the decomposition of π-complexes, with carbon tetrachloride and metal clusters formed in the system. At substantially lower CCl_4 concentrations, the decomposition of π-complexes was accompanied by the preferential aggregation of atoms to form nanosized silver clusters, which were stabilised in the matrix up to a temperature corresponding to the system restructuring, *i.e.*, 210–230 K. It is noteworthy that the CESR signals of nanosized silver clusters were more symmetric for ternary co-condensates Ag/5CB/CCl_4 as compared with the binary Ag/5CB system. This may serve as evidence for the narrowing of the size distribution of metal clusters. Apparently, the observed effect was caused by the fact that the least stable and most reactive clusters were the first to react; the most stable and highly symmetrical icosahedral clusters (Ag_{13}, Ag_{55}, *etc.*) were stabilised in the 5CB matrix and accumulated at this temperature. Thus, at low temperatures, the role of active species in the reaction with CCl_4 was played by silver atoms; on heating of the co-condensate, the nanosized clusters, which were formed in the aggregation of the silver atoms emerged in the thermal decomposition of complexes, also became reactive.

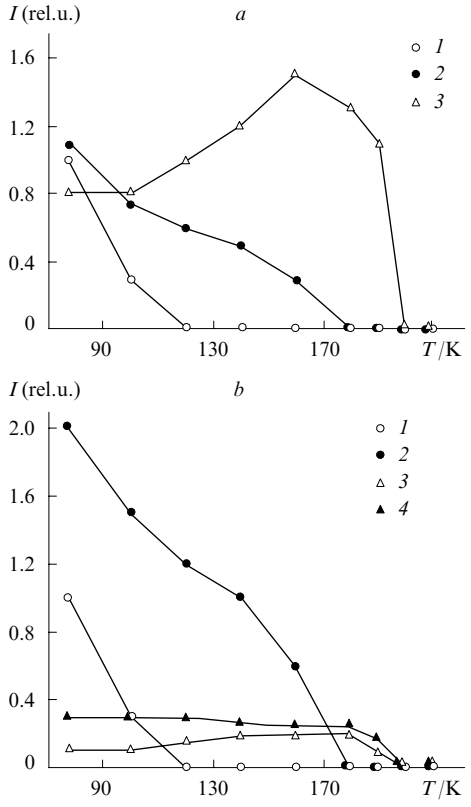


Figure 13. Temperature dependences of relative intensities of paramagnetic signals of the reaction products of silver atoms and clusters with carbon tetrachloride and matrix (5CB) molecules for co-condensates with reactant ratios (*a*) Ag : CCl_4 : 5CB = 1 : 3 : 100 and (*b*) 1 : 10 : 100.[125] (*1*) $Ag(5CB)_2$, (*2*) $ClAgCCl_3$, (*3*) Ag_x, (*4*) $Ag(5CB)CCl_4$.

Gold is conventionally classified with the most stable and least reactive metals the surface of which is inert with respect to chemisorption of molecules of most gases.[126] Gold is the only transition metal that does not have a stable oxide (its most stable oxide, Au_2O_3, is actually metastable). Gold exhibits the maximum electronegativity among all metals, being only slightly more positive as compared with typical non-metals such as sulfur or iodine; gold has the record-breaking electron affinity (2.31 eV) and ionisation potential (9.22 eV).[127]

In the past decade, gold particles measuring < 5 nm attracted attention due to their unique catalytic properties.[128–133] It was shown that gold clusters and nanoparticles are efficient catalysts in low-temperature CO oxidation,[131, 132] selective propene oxidation to propene oxide,[134] NO reduction,[135] selective hydrogenation of acetylene and butadiene,[136] reduction of nitrogen oxides,[137] hydrochlorination of acetylene to vinyl chloride,[138, 139] vinyl acetate synthesis[140] and some other reactions.[141, 142]

Low-temperature (10 K) co-condensation of gold atoms with a CO and O_2 mixture (1 : 1) was found to produce gold(II) carbonyl peroxyformate. The latter underwent decomposition to two CO_2 molecules when heated to 30–40 K.[143] Thus, it can be concluded that the carbon monoxide oxidation to dioxide CO_2 is catalysed by individual gold atoms.

It was stated that Au_2 dimers react with CO, NH_3 and ethylene.[144] In contrast to silver and copper dimers, gold dimers reacted with molecular hydrogen, which may be associated with the relativistic nature of gold. This determines the contraction of s orbitals to make the resulting Au–H bond more stable.

Using a mass-selection technique and jet reactors, the molecular adsorption of different molecules on neutral and charged gold clusters Au_x, Au_x^-, Au_x^+ ($x = 2-20$) was studied.[145–147] For anionic clusters involving up to 20 atoms, a 'saw-tooth' size dependence of oxygen adsorption with a clearly pronounced even-odd alternation was observed.[147, 148] Clusters containing even numbers of atoms readily adsorbed oxygen, whereas those with odd number of atoms were inert. This effect was due to the strong alternation of the electron affinity with the varied cluster size. The higher electron affinity for clusters with odd numbers of atoms[146] prevented the adsorption of oxygen molecules that occurs due to the electron density transfer from a gold cluster to the antibonding π* orbital of the oxygen molecule.[148] Gold species with the number of atoms > 20 were far less reactive.

The chemisorption of carbon monoxide on anionic gold clusters led to preferential formation of mono- and dicarbonyl clusters with odd numbers of gold atoms, namely, Au_5CO, $Au_{11}CO$, $Au_{15}CO$, $Au_{15}(CO)_2$.[149, 150] Even the long-term exposure of this system at high CO concentrations did not lead to the formation of higher carbonyls. This agrees with the

earlier data on the CO adsorption on the surface of gold single crystals for which the adsorption curves reached saturation at small surface coverages. It is interesting that a single-atom gold anion did not virtually react with CO, whereas one or two CO molecules reacted with dimeric (Au_2^-) and trimeric (Au_3^-) gold anions to preferentially afford $Au_3(CO)_2$ dicarbonyl in a stable 8-electron configuration.[151] This also involved a shift of s and d orbitals of a gold atom as a manifestation of the relativistic effects.

Studies of oxygen and CO chemisorption play an important role for efficient CO oxidation to CO_2. Co-chemisorption of oxygen and CO was successfully performed on anions of gold dimers (Au_2^-) and trimers (Au_3^-); no adsorption was observed on monomeric anions Au^- (see Ref. 152). No formation of gold carbonyls was detected in the reaction with oxygen that proceeded an order of magnitude faster than the CO adsorption. Among intermediate products, $Au_3(CO)O_2$ and $Au_3(CO)(O_2)$ were detected, which confirmed the co-adsorption. The initial CO adsorption on Au_6^- clusters led to the formation of several carbonyls $Au_6(CO)_n$. Subsequent treatment of these clusters with oxygen resulted in the ligand substitution to form $Au_6(CO)_{n-1}O_2^-$, where one CO molecule underwent oxidation to CO_2. For gold clusters, the reaction rate exceeded that observed on common gold catalysts by at least two orders of magnitude. The disadvantage of using such small particles concerns the impossibility of recycling this catalytic system.[153]

The reaction of gold dimer anion Au_2^- with CO and O_2 led to the formation of $Au_2O_2^-$ and $Au_2(CO)O_2^-$; the final system contained also Au_2^- species.[154] The following scheme of oxidation was assumed:

$$Au_2^- + O_2 \longrightarrow Au_2O_2^-,$$

$$Au_2O_2^- + CO \longrightarrow Au_2(CO)O_2^-,$$

$$Au_2(CO)O_2^- + CO \longrightarrow Au_2^- + 2CO_2.$$

Density functional theory calculations pointed to a possibility of the existence of an intermediate species $Au_2(CO)O_2^-$ both as the product of CO insertion into the O–O bond (Fig. 14 *a*) and in the form of gold dimer peroxyformate (Fig. 14 *b*), which opens up a virtually activationless route of $Au_2O_2^-$ reaction with CO.[153, 154]

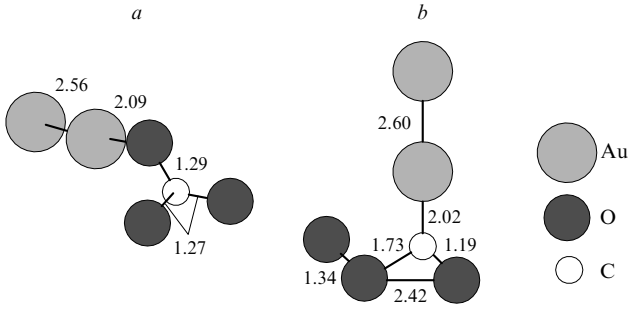


Figure 14. Reaction products of CO and O_2 with gold clusters (bond distances are shown in Å);
(*a*, *b*) see text.[154]

Fourier-transform mass spectrometry and ion-cyclotron resonance studies of the O_2 and CO co-chemisorption on gold nanoclusters have unambiguously demonstrated that the preliminary treatment with CO considerably accelerated the reaction of the cluster with O_2. This pointed to the cooperative effect of two ligands on the CO oxidation.[155] In this process, both the reaction with Au_n^- gold anions and the oxidation of preliminarily formed carbonyl complexes $Au_n(CO)_m$ were size-sensitive. Carbon dioxide was the product of both reactions.

The presence of water vapour had a considerable effect on the reactivity of gold clusters Au_n. As compared with the original clusters, the hydroxylated Au_nOH^- clusters formed upon oxidation exhibited the inverse reactivity, namely, clusters with an even number n were inert and those with an odd numbers easily chemisorbed oxygen.[156]

The reactivity of Au_n^+ ($n = 1-12$) clusters in their reactions with H_2S was studied.[157] Cations Au^+ and Au_2^+ were virtually inert; among larger species, clusters with even n were more reactive. The reaction led to the liberation of hydrogen and formation of sulfur-containing products. Cationic clusters with the number of gold atoms up to 10 efficiently chemisorbed hydrogen.

The reactivity of large gold clusters ($n \geqslant 10$) depended on their structure and shape.[158, 159] Modelling of structures of nanosized gold clusters both anionic and neutral has shown[160–162] that due to the contribution of relativistic factors, gold species (containing up to 13 atoms) had the shape of a plane or a plate. Moreover, the ionisation potential, the electron affinity, the difference in energies of the highest occupied and the lowest unoccupied molecular orbitals, and the ability to selectively chemisorb molecules of O_2, CO, *etc.* are all the size-dependent quantities that exhibit the typical alternation for clusters containing even and odd numbers of metal atoms.[163, 164] For planar gold species, substantial anisotropy of polarisability was observed.[165] In the lateral direction, the polarisability was high (close to that of metals), whereas in the normal direction, the polarisability value approached that of semiconducting silicon. The theoretical prediction of structures for species with $n = 30-10\,000$ has demonstrated the possibility of formation of different types of disordered,[166] edged cuboctahedral and icosahendal clusters[167–169] that could be transformed to one another[170] due to small difference in stabilisation energies.[166]

In catalysis, nanosized gold clusters and particles deposited on metal-oxide supports were used.[171–174] Several studies were devoted to the formation of gold nanoparticles in the vapour deposition from the gas phase to afford two- and three-dimensional aggregates.[175–177] It was shown that the activity of deposited nanodispersed gold particles is largely determined by the interaction of metal particles with the substrate, the presence of adsorbed and covalently bound functional groups, the electron-donating or -withdrawing properties of the surface, the size of deposited particles and the presence of low-coordinated gold atoms in their structure as well as by the degree of charge transfer in the chemisorption of a reagent molecule.[178–180] A strong size effect was observed in the CO oxidation to CO_2 on the exposure of a $CO:O_2 = 1:5$ mixture over deposited Au/TiO_2 clusters at room temperature. The maximum activity was observed for gold particles measuring 2.8–3.2 nm (Fig. 15). This was associated with the transformation of particles that exhibit non-metal properties into particles with metallic properties.[181] A detailed analysis of the effect of the size and the shape of gold particles deposited on different substrates was performed.[182] The properties of deposited gold nanoparticles were observed to widely deviate from those of bulk gold samples, *e.g.*, the activity deviated by more than an order of magnitude.[183, 184] Highly symmetric (with a fifth-order symmetry axis) gold clusters with 'magic' numbers of atoms, namely, 13, 55, 147, *etc.*, proved to be more stable and less reactive. Thus an Au_{55} cluster ($d = 1.4$ nm) was unsusceptible to oxidation under the action of oxygen plasma, whereas smaller clusters (< 1 nm) underwent oxidation under these conditions.[185]

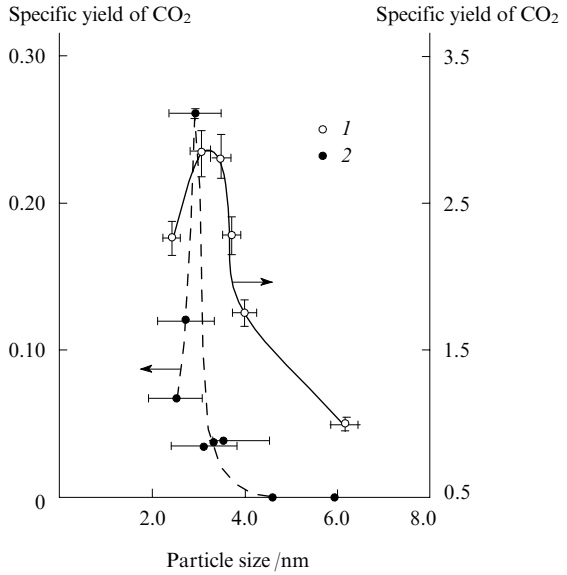


Figure 15. Activity of gold particles deposited on TiO_2 by (*1*) vacuum condensation and (*2*) chemical deposition as a function of their size.[129]

VI. Conclusion

This survey of the literature data and of the results obtained by the authors of this review shows that the methods of cryochemistry and nanochemistry make it possible to carry out and control self-assembling processes of metal atoms to form nano- and subnanosized aggregates, perform competitive chemical reactions of atoms, small clusters and nanosized particles of transition metals with different organic and inorganic substances, study the kinetics of cryochemical process and simulate their individual stages, and acquire information on the mechanisms of uncommon chemical reactions in low-temperature co-condensates.

At present, effective low-temperature methods are being developed aimed at the stabilisation of small clusters and nanosized metal particles in the matrices formed by inert gases and certain organic and inorganic substances and on the surfaces of different substrates and at carrying out selective chemical reactions of particles of different sizes and shapes with reagents added to the systems. The accumulation of data on the reactions of nanosized particles of different metals for a wide range of temperatures in the gas phase and in condensed systems, namely, liquid and solid co-condensates, as well as their kinetic analysis will allow one to reveal the fundamental trends in the manifestation of size effects in nanochemistry of metals and the periodicity in the variation of reactivity of these particles. This information together with the comparative analysis of characteristics of ligand-free and ligand-stabilised clusters makes it possible to separate the effect of the metal core size and the stabilising effect of the ligand shell and the effects of the phase state of the system and its temperature. This approach coupled with the quantum chemical modelling of the studied systems will allow one to pass from documentation of separate cases of the dependence of the particle reactivity on the number of the constituent atoms to the development of the general kinetic theory that would relate the particle size in the studied substances to their chemical properties. Cryonanochemistry is used in the elaboration of new methods for the synthesis of nanostructurised materials with unique optical, magnetic, electrophysical and mechanical characteristics.

It is also necessary to mention certain general problems that challenge modern cryonanochemistry. First of all, this is the development of methods of synthesis of metal particles with controlled sizes and narrow size distributions in the range of 1 – 5 nm. The synthesis of highly reactive nanoparticles requires the elaboration of special effective methods for their stabilisation.

Second, it is necessary to develop methods for carrying out highly selective catalytic, photochemical and thermal processes based on competitive reactions of small metal particles to be used as the basis in the production of nanodevices and nanomaterials. The quest for promising applications is associated with the development of methods for the formation of ordered ensembles of metal particles of definite sizes and shapes incorporated into the structurised matrices based on polymers, liquid crystals, carbonaceous and biological systems. The use of low temperatures offers a possibility of the direct introduction of metal atoms and clusters into organic and inorganic matrices without using additional chemical reagents and solvents. This can result in the development of environmentally clean and safe methods for the synthesis of nanostructurised materials.

Third, the carrying out of cryonanochemical processes and the synthesis of nanoparticles and nanostructurised materials to be used in practice should be accompanied by scaling of synthetic methods to obtain the required macroamounts of target products and by the development of procedures for maintaining long-term stability of their physical and chemical properties.

Wide prospects are opened up for the use of cryochemical methods in the production of metal-containing nanostructures on cooled surfaces of organic, inorganic and polymeric substances. The use of low temperatures and the controlled condensation of reagent vapour allow one to synthesise and stabilise particles measuring 1 nm and smaller. Such hybrid materials may find their application in catalysis and as chemical sensors.

Of undeniable interest is the development of multifunctional hybrid nanosystems based on chemically modified metal particles and biologically active substances, which includes the development of new systems for medicinal diagnostics and the target delivery of medicinal drugs.

This review was financially supported by the Russian Foundation of Basic Research (Project Nos 04-03-32 748 and 05-03-32 293) and the INTAS programme (Grant No. 2000-00 911).

References

1. G B Sergeev *Nanochemistry* (Amsterdam, Boston, Heidelberg, London, New York, Oxford, Paris, San Diego, San Francisko, Singapore, Sydney, Tokyo: Elsevier, 2006)
2. G B Sergeev *J. Nanopart. Res.* **5** 529 (2003)
3. T I Shabatina, G B Sergeev *Usp. Khim.* **72** 643 (2003) [*Russ. Chem. Rev.* **72** 571 (2003)]
4. G B Sergeev, T I Shabatina *Surf. Sci.* **500** 628 (2002)
5. K J Klabunde *Free Atoms, Clusters and Nanoscale Particles* (San Diego, New York, Boston, London, Sydney, Tokyo: Academic Press, 1994)
6. G B Sergeev *Usp. Khim.* **70** 915 (2001) [*Russ. Chem. Rev.* **70** 809 (2001)]
7. W Leitner *Coord. Chem. Rev.* **153** 257 (1996)
8. D H Gibson *Chem. Rev.* **96** 2063 (1996)
9. A Behr *Carbon Dioxide Activation by Metal Complexes* (Weinheim: VCH, 1988)
10. M Aresta, E Quaranta, I Tomassi *New J. Chem.* **18** 133 (1994)
11. P Brounstein, D Matt, D Nobel *Chem. Rev.* **88** 747 (1988)
12. J Mascetti, F Galan, I Papai *Coord. Chem. Rev.* **190 – 192** 557 (1999)
13. F Galan, M Fouassier, M Tranquille, J Mascetti, I Papai *J. Phys. Chem. A* **101** 2626 (1997)
14. J Mascetti, R Fournier, I Papai *J. Phys. Chem. A* **101** 4465 (1997)

15. C Jegat, J Mascetti *New J. Chem.* **15** 17 (1991)
16. Y K Lee, Y Hannachi, C Xu, L Andrews, L Manceron *J. Phys. Chem.* **100** 11228 (1996)
17. F Bernardi, A Bottoni, M Calcinari, I Rossi, M A Robb *J. Phys. Chem.* **101** 6316 (1997)
18. K Pierloot, B J Persson, B O Roos *J. Phys. Chem.* **99** 3465 (1995)
19. T H Upton, W A Goodbart *J. Am. Chem. Soc.* **100** 321 (1978)
20. T Merle-Mejean, C Cosse-Merteas, S Bouchareb, F Galan, J Mascetti, M Tranquille *J. Phys. Chem.* **96** 9148 (1992)
21. Yu K Lee, L Manceron, I Papai *J. Phys. Chem. A* **101** 9650 (1997)
22. G V Chertihin, L Andrews *J. Am. Chem. Soc.* **116** 8322 (1994)
23. Z Xiao, R H Hauge, J L Margrave *J. Phys. Chem.* **95** 2696 (1991)
24. J Mascetti, M Tranquille *J. Phys. Chem.* **92** 2177 (1988)
25. G V Chertihin, L Andrews *J. Am. Chem. Soc.* **117** 1595 (1995)
26. C Jegat, M Fouassier, M Tranquille, J Mascetti *Inorg. Chem.* **30** 1529 (1991)
27. C Jegat, M Fouassier, J Mascetti, M Tranquille, I Tomassi, M Aresta, F Ingold, A Dendieu *Inorg. Chem.* **35** 4254 (1996)
28. Y Hannachi, J Mascetti, A Stirling, I Papai *J. Phys. Chem. A* **107** 6708 (2003)
29. F Elustondo, J Mascetti, I Papai *J. Phys. Chem. A* **104** 3572 (2000)
30. Y Dobrogorskaya, J Mascetti, I Papai, A Nemukhin, Y Hannachi *J. Phys. Chem. A* **107** 2711 **(**2003)
31. Y Dobrogorskaya, J Mascetti, A Nemukhin, I Papai, Y Hannachi *J. Phys. Chem. A* **109** 7932 (2005)
32. Y Dobrogorskaya, J Mascetti, Y Hannachi *J. Phys. Chem. A* **111** (2008) (in the press)
33. T L Haslett, S Fedrigo, K Bosnick, M Moskovits, H A Duarte, D Salahub *J. Am. Chem. Soc.* **122** 6039 (2000)
34. F Elustondo, Ph.D. Thesis Université Bordeaux 1, Bordeaux, 1997
35. V T Aleksanyan, B V Lokshin *Stroenie Molekul i Khimicheskaya Svyaz' (Itogi Nauki i Tekhniki)* [Structure of Molecules and Chemical Bond (Advances in Sciences and Engineering)] (Moscow: Izd. VINITI, 1976) Vol. 5, p. 178
36. B V Lokshin *Proceedings of the 6th International Conference on Low Temperature Chemistry, Chernogolovka, 2006* p. 45
37. B V Lokshin, I I Greenwald *J. Mol. Struct.* **220** 11 (1990)
38. T S Kurtikyan, G M Gulyan, A A Hovhannisyan, N A Gabrielyan *Proceedings of the 6th International Conference on Low Temperature Chemistry, Chernogolovka, 2006* p. 44
39. M Dalibart, J Derouault *J. Mol. Struct.* **218** 1 (1990)
40. T R Gebale, T Oka *Nature (London)* **384** 334 (1996)
41. T R Geballe, B J Mc Call, K H Hinkle, T Oka *Astrophys. J.* **510** 251 (1999)
42. M Cordonier, D Uy, R M Dickson, K E Kerr, Y Zang, T Oka *J. Chem. Phys.* **113** 318 (2000)
43. S Tam, M E Fajardo, H Katsuki, H Hoshina, T Wakabayashi, T Momose *J. Chem. Phys.* **111** 4191 (1999)
44. T Momose, M Miki, T Wakabayashi, T Shida, M C Chan, S S Lee, T Oka *J. Chem. Phys.* **107** 7707 (1997)
45. R J Hinde, D T Anderson, S Tam, M E Fajardo *Chem. Phys. Lett.* **356** 355 (2002)
46. S I Kiselev, V V Khmelenko, D M Lee, V Kiryuhin, R E Boltnev, E B Gordon, B Keimer *Phys. Rev., B* **65** 024517 (2002)
47. S I Kiselev, V V Khmelenko, C Y Lee, D M Lee *J. Low Temp. Phys.* 128 (2002)
48. E G Kisvarsanyi, N S Sullivan *Phys. Rev. B* **48** 16577 (1993)
49. F Elustondo, M Dalibart, J Derouault, J Mascetti *Phys. Chem. Earth* **24** 583 (1999)
50. M Moskovits, G Ozin *Cryochemistry* (New York: Wiley, 1976)
51. W Harbig, S Fedrigo, S Buttet, D Lindsay *J. Chem. Phys.* **96** 8104 **(**1992**)**
52. G A Ozin, A C Arsenault *Nanochemistry. A Chemical Approach to Nanochemistry* (Cambridge: RSC, 2005)
53. *Nanoparticles from Theory to Applications* (Ed. G Schmid) (Weinheim: VCH, Wiley, 2005)
54. B M Sergeev, G B Sergeev, A N Prusov *Mendeleev Commun.* 68 (2001)
55. B M Sergeev, G B Sergeev, V A Kasaikin, E A Litmanovich, A N Prusov *Mol. Cryst. Liq. Cryst.* **356** 121 (2001)
56. G Yu Yurkov, A V Kozinkin, T I Nedoseikina, A T Shuvaev, V G Vlasenko, S P Gubin, I D Kosobudskii *Neorg. Mater.* **37** 1175 (2001) [a]
57. G B Sergeev, V V Zagorskii, M A Petrukhina *J. Mater. Chem.* **5** 31 (1995)
58. G B Sergeev, M A Petrukhina *Prog. Solid State Chem.* **24** 183 (1996)
59. L I Trahtenberg, G N Gerasimov *Metal-Polymer Nanocomposites* (Eds L Nicolais, G Carotenuto) (New York: Wiley, 2005) p. 37
60. G B Sergeev, V V Zagorskii, M A Petrukhina, S Zaviyalov, E Grigoriev, L Trachtenberg *Anal. Commun.* **34** 113 (1997)
61. V E Bochenkov, N Stephan, L Brehmer, V V Zagorskii, G B Sergeev *Colloids Surf. A* **198**–**200** 911 (2002)
62. V M Kozhevin, D A Yavsin, S A Gurevich, T N Rostovshikova, V V Smirnov *Ros. Nanotekhnol.* **2** 47 (2007) [b]
63. P S Vorontsov, E I Grigor'ev, S A Zav'yalov, L M Zav'yalova, T N Rostovshchikova, O V Zagorskaya *Khim. Fiz.* **21** 45 (2002) [c]
64. T I Shabatina *Vestn. Mosk. Univ., Ser. 2, Khim.* **43** 273 (2002) [d]
65. T I Shabatina, E V Vovk, V A Timoshenko, Yu N Morosov, G B Sergeev *Colloids Surf. A* **198**–**200** 255 (2002)
66. T I Shabatina, V A Timoshenko, A A Belyaev, Yu N Morozov, G B Sergeev *Dokl. Akad. Nauk* **387** 219 (2002) [e]
67. T I Shabatina *Struct. Chem.* **18** 511 (2007)
68. T I Shabatina, V A Timoshenko, Yu N Morosov, G B Sergeev *Mater. Sci. Eng., C* **22** 193 (2002)
69. T I Shabatina, E V Vovk, Yu N Morosov, V A Timoshenko, G B Sergeev *Mol. Cryst. Liq. Cryst.* **356** 143 (2001)
70. T I Shabatina, V A Timoshenko, Yu N Morosov, G B Sergeev *Mol. Cryst. Liq. Cryst.* **390** 43 (2003)
71. N V Ozhegova, T I Shabatina, A V Nemukhin, G B Sergeev *Mendeleev Commun.* 218 (1998)
72. T I Shabatina, E V Vovk, N V Ozhegova, Yu N Morosov, A V Nemukhin, G B Sergeev *Mater. Sci. Eng.* **8**–**9** 53 (1999)
73. J A Howard, H A Joly, D Mile *J. Phys. Chem.* **94** 1275 (1990)
74. A J Buck, B Mile, J A Howard *J. Am. Chem. Soc.* **105** 3381 (1983)
75. V A Timoshenko, A A Belyaev, Yu N Morosov, T I Shabatina, G B Sergeev *Mol. Cryst. Liq. Cryst.* **440** 79 (2005)
76. J H Michalik, D Yamada, R Brown, L Kevan *J. Phys. Chem.* **100** 4213 (1996)
77. G Mitrikas, Y Deligiannakis, C C Trapalis, N Boukos, G Kordas *J. Sol-Gel Sci. Technol.* **13** 503 (1998)
78. E V Polikarpov, T I Shabatina, G B Sergeev, A V Nemukhin *Vestn. Mosk. Univ., Ser. 2, Khim.* **41** 283 (2000) [d]
79. U Kreibig, M Volmer *Optical Properties of Metal Clusters* (Berlin: Springer, 1995) p. 532
80. T I Shabatina *Zhidkie Kristally i Ikh Prakticheskoe Ispol'zovanie* (Liquid Crystals and Their Practical Use) (Ivanovo: Ivanovo State University, 2002) Vol. 1, p. 58
81. T I Shabatina, G B Sergeev *Fizikokhimiya Ul'tradispersnykh Nanosistem* (Physical Chemistry of Ultradisperse Nanosystems) (Moscow: Moscow Engineering Physical Institute, 2005) p. 108
82. F G N Cloke *Chem. Soc. Rev.* 17 (1993)
83. P L Arnold, M A Petrukhina, V E Bochenkov, T I Shabatina, V V Zagorskii, G B Sergeev, F G N Cloke *J. Organomet. Chem.* **688** 49 (2003)
84. L Maron, O Eisenstein *J. Phys. Chem. A* **104** 7140 (2000)
85. S A Konnov, L V Serebrennikov, A A Mal'tsev *Zh. Neorg. Khim.* **27** 654 (1982) [f]
86. R L DeKock, W Weltner Jr *J. Phys. Chem.* **75** 514 (1971)
87. N S Loktyushina, S B Osin, A A Mal'tsev *Zh. Neorg. Khim.* **29** 1718 (1984) [f]
88. N S Loktyushina, S B Osin *Zh. Neorg. Khim.* **32** 2918 (1987) [f]
89. V N Solov'ev, Candidate Thesis in Chemical Sciences, Moscow State University, Moscow, 1998
90. G B Sergeev, T I Shabatina, V N Solov'ev, A V Nemukhin *Spectrochim. Acta, A* **56** 2527 (2000)
91. G B Sergeev, V V Zagorskii, M V Grishechkina *Vestn. Mosk. Univ., Ser. 2, Khim.* **29** 583 (1988) [d]
92. G B Sergeev, V V Zagorskii, M V Grishechkina *Metalloorg. Khim.* **1** 820 (1988) [g]
93. V V Zagorsky, G B Sergeev *Mol. Cryst. Liq. Cryst.* **186** 81 (1990)
94. J M Carretas, A Pires de Matos *Mater. Chem. Phys.* **31** 123 (1992)

95. V V Zagorskii, S E Kondakov, A M Kosolapov, G B Sergeev, V N Solov'ev *Metalloorg. Khim.* **5** 533 (1992) [g]
96. G B Sergeev, V V Zagorskii, A M Kosolapov, S E Kondakov *Metalloorg. Khim.* **8** 3212 (1995) [g]
97. F G N Cloke, H C de Lemos, A A Sameh *J. Chem. Soc., Chem. Commun.* 1344 (1986)
98. W J Evans, S C Engerer, A C Neville *J. Am. Chem. Soc.* 331 (1978)
99. W J Evans, K M Coleson, S C Engerer *Inorg. Chem.* **20** 4320 (1981)
100. W J Evans, S C Engerer, K M Coleson *J. Am. Chem. Soc.* **103** 6672 (1981)
101. W J Evans *Polyhedron* **6** 803 (1987)
102. I G Tarkhanova, Candidate Thesis in Chemical Sciences, Moscow State University, Moscow, 1990
103. V V Zagorskii, S E Kondakov, A M Kosolapov *Vestn. Mosk. Univ., Ser. 2, Khim.* **33** 249 (1992) [d]
104. J L Slater, T C De Vore, V Calder *Inorg. Chem.* **13** 1808 (1974)
105. J L Slater, T C De Vore, V Calder *Inorg. Chem.* **12** 1918 (1973)
106. W E Klotzbucher, M A Petrukhina, G B Sergeev *Mendeleev Commun.* 5 (1994)
107. M P Andrews, A L Wayda *Organometallics* **7** 743 (1988)
108. V E Bochenkov, V V Zagorskii, G B Sergeev *Vestn. Mosk. Univ., Ser. 2, Khim.* **41** 327 (2000) [d]
109. W A King, T J Marks, D M Anderson, D J Duncalf, F G N Cloke *J. Am. Chem. Soc.* **114** 9221 (1992)
110. A V Vlasov, T I Shabatina, A Yu Ivanov, G G Sheina, A V Nemukhin, G B Sergeev *Mendeleev Commun.* 10 (2005)
111. T I Shabatina, A V Vlasov, G B Sergeev *Mol. Cryst. Liq. Cryst.* **356** 149 **(**2001)
112. T I Shabatina, A V Vlasov, E V Vovk, D J Stufkens, G B Sergeev *Spectrochim. Acta, A* **56** 2539 (2000)
113. T I Shabatina, A V Vlasov, G B Sergeev *Mater. Sci. Eng., C* **22** 373 (2002)
114. A V Vlasov, I N Zelikov, T I Shabatina, G B Sergeev *Mol. Cryst. Liq. Cryst.* **390** 35 (2003)
115. A V Vlasov, T I Shabatina, S V Konyukhov, A Yu Ermilov, A V Nemukhin, G B Sergeev *Zh. Strukt. Khim.* **45** 406 (2004) [h]
116. T I Shabatina, A V Vlasov, S V Konyuhov, A Yu Ermilov, A V Nemukhin, G B Sergeev *Mol. Cryst. Liq. Cryst.* **440** 317 (2005)
117. T I Shabatina, A V Vlasov, A Yu Ermilov, S V Konyukhov, A V Nemukhin, G B Sergeev *Zh. Strukt. Khim.* **48** 814 (2007) [h]
118. A V Vlasov, T I Shabatina, G B Sergeev *Zh. Fiz. Khim.* **76** 1965 (2002) [i]
119. A V Vlasov, Candidate Thesis in Chemical Sciences, Moscow State University, Moscow, 2006
120. N M Emanuel', A L Buchachenko *Khimicheskaya Fizika Razrusheniya i Stabilizatsii Polimerov* (Chemical Physics of Destruction and Stabilisation of Polymers) (Moscow: Nauka, 1988) p. 368
121. G B Sergeev *Mol. Cryst. Liq. Cryst.* **440** 85 (2005)
122. G B Sergeev, T I Shabatina *Colloids Surf. A* (2008) (in the press)
123. V A Timoshenko, T I Shabatina, Yu N Morosov, G B Sergeev *Appl. Surf. Sci.* **246** 420 (2005)
124. T I Shabatina, Yu N Morosov, V A Timoshenko, G B Sergeev *Mol. Cryst. Liq. Cryst.* **440** 325 (2005)
125. V A Timoshenko, T I Shabatina, Yu N Morozova, G B Sergeev *Zh. Strukt. Khim.* **47** 146 (2006) [h]
126. M Haruta *Catal. Today* **36** 153 (1997)
127. D F Shriver, P A Atkins *Inorganic Chemistry* (Oxford: Oxford University Press, 1999)
128. M-C Daniel, D Astruc *Chem. Rev.* **104** 293 (2004)
129. R Meyer, C Lemire, Sh K Shaikhutdinov, H-J Freund *Gold Bull.* **37** 72 (2004)
130. S Schimpf, M Lucas, C Mohr, U Rodemerk, A Brukner, J Radnik, H Hofmeister, P Claus *Catal. Today* **72** 63 (2002)
131. D T Thompson *Appl. Catal., A* **243** 201 (2003)
132. M M Schubert, S Hacjenberg, A C Van Vee, M Muhler, V Plzak, R Behm *J. Catal.* **197** 113 (2001)
133. L Fan, N Ichikuni, S Shimadzu, T Uematsu *Appl. Catal.* **246** 87 (2003)
134. T Hayashi, K Tanaka, M Haruta *J. Catal.* **178** 566 (1998)
135. M A Banares *Catal. Today* **100** 71 (2005)
136. A Ueda, M Haruta *Gold Bull.* **32** 3 (1999)
137. H Sakuri, M Haruta *Catal. Today* **29** 361 (1996)
138. A Ueda, T Oshima, M Haruta *Appl. Catal., B* **12** 81 (1997)
139. G Hutchings *Catal. Today* **72** 11 (2002)
140. T V Choudhary, D W Goodman *Catal. Today* **77** 65 (2002)
141. A S K Hashimi *Gold Bull.* **36** 3 (2003)
142. V V Smirnov, S N Lanin, A Yu Vasil'kov, S A Nikolaev, G P Murav'eva, L A Tyurina, E V Vlasenko *Izv. Akad. Nauk, Ser. Khim.* 2215 (2005) [j]
143. L Lian, P A Hackett, D M Rayner *J. Phys. Chem.* **99** 2583 (1993)
144. J Li, X Li, H J Zhai, L S Wang *Science* **299** 864 (2003)
145. B E Salisbury, W T Wallance, R L Whetten *Chem. Phys.* **262** 131 (2000)
146. D Stolcic, M Fisher, G Gantefor, Y D Kim, Q Sun, P Jena *J. Am. Chem. Soc.* **125** 2848 (2003)
147. Y D Kim, M Fisher, G Gantefor *Chem. Phys. Lett.* **377** 170 (2003).
148. S A C Carabineiro, D T Tompson *Nanocatalysis* (Eds U Heinz, U Landman) (Berlin: Springer, 2007) p. 37
149. W T Wallace, R L Whetten *J. Phys. Chem. B* **104** 10964 (2000)
150. W T Wallace, R L Whetten *Eur. Phys. J. D* **16** 123 (2001)
151. J Hagen, L D Socaciu, U Heiz, T M Bemhardt, L Woste *Eur. Phys. J. D* **24** 327 (2003)
152. J Hagen, L D Socaciu, M Elijazyfer, U Heiz, T M Bemhardt, L Woste *Phys. Chem. Chem. Phys.* **4** 1707 (2002)
153. W T Wallace, R L Whetten *J. Am. Chem. Soc.* **124** 7499 (2002)
154. L D Socaciu, J Hagen, T M Bemhardt, L Woste, U Heiz, H Hakkinen, U Landman *J. Am. Chem. Soc.* **125** 10437 (2003)
155. I Balteanu, O P Balaj, B S Fox, M K Beyer, Z Bastl, V E Bondybey *Phys. Chem. Chem. Phys.* **5** 1213 (2003)
156. W T Wallace, R B Wrywas, R L Whetten, R Mitric, V Bonacic *J. Am. Chem. Soc.* **125** 8408 (2003)
157. K Sugawa, F Sobbot, A V Vakhtin *J. Chem. Phys.* **118** 7808 (2003)
158. B Hammer, J Norskov *Nature (London)* **376** 238 (1995)
159. M Mavrikakis, P Stoltze, J Norskov *Catal. Lett.* **64** 101 (2001)
160. H Hakkinen, B Yoon, U Landman, X Li, H J Zhai, L S Wang *J. Phys. Chem. A* **107** 6168 (2003)
161. J Wang, G Wang, J Zhao *Phys. Rev., B* **66** 035418 (2002)
162. N Lopez, J K Norskov *J. Am. Chem. Soc.* **124** 11262 (2002)
163. B Yoon, H Hakkinen, U Landman *J. Phys. Chem. A* **107** 4066 (2003)
164. H Gronbek, W Andreoni *Chem. Phys.* **262** 1 (2000)
165. I L Garzon, K Michaelian, M R Beltranm, A Posada-Amarillias, P Ordejon, E Artacho, D Sanchez-Portal, J M Soler *Eur. Phys. J. D* **9** 211 (1999).
166. C L Cleveland, U Landman, M N Shafigullin, P W Stephens, R L Whetten *Z. Phys. D: At., Mol. Clusters* **40** 503 (1997)
167. C L Cleveland, U Landman, T G Schaff, M N Shafigullin, P W Stephens, R L Whetten *Phys. Rev. Lett.* **79** 1873 (1997)
168. G Mills, M S Gordon, H Metiu *Chem. Phys. Lett.* **359** 493 (2002)
169. S A Varganov, R M Olson, M S Gordon, H Metiu *J. Chem. Phys.* **119** 2531 (2003)
170. P Gunter, J W Niemantsverdriet, F Ribiero, G Somorjai *Catal. Rev. Sci. Eng.* **38** 77 (1997)
171. H J Freund, M Baumer, H Kuhlenbeck *Adv. Catal.* **45** 333 (2000)
172. H J Freund *Surface Sci.* **500** 271 (2002)
173. U Diebold *Surface Sci. Rep.* **48** 53 (2003)
174. L Zhang, R Persaud, T E Madey *Phys. Rev. B* **56** 10549 (1997)
175. T Bredow, G Pacchioni *Chem. Phys. Lett.* **355** 417 (2002)
176. X Lai, T P S Lclair, M Valden, D W Goodman *Prog. Surf. Sci.* **59** 25 (1998)
177. N Lopez, T V W Janssens, B S Clausen, Y Xu, M Mavrikakis, T Bligaard, J K Norskov *J. Catal.* **223** 232 (2004)
178. J A Rodriguez, M Perez, T G Jirsak, J Evans *J. Chem. Phys. Lett.* **378** 526 (2003)
179. C L Bianchi, S Biella, A Gervasini, L Prati, M Rossi *Catal. Lett.* **85** 91 (2003)

180. A K Santra, D W Goodman *J. Phys.: Condens. Matter* **14** R31 (2002)
181. T V W Janssens, A Carlsson, A Puig-Molina, B S Clausen *J. Catal.* **240** 108 (2006)
182. B Hvolback, T V W Janssens, B S Clausen, C H Christensen, J K Norskov *Nano Today* **2** 14 (2007)
183. Y J Zhu, A Schnieders, J D Alexander, T P Beebe *Langmuir* **18** 5728 (2002).
184. H G Boyen, G Kastle, F Wiegl, B Kozlowski, C Dietrich, P Ziemann, J P Spatz, S Riethmuller, C Hartmann, M Moeller, G Schmid, M C Garnier, P Oelhafen *Science* **297** 1533 (2002)
185. H Zhang, G Schmid, U Hartmann *Nano Lett.* **3** 305 (2003)

[a] — *Inorg. Mater. (Engl. Transl.)*
[b] — *Nanotechnol. Russ. (Engl. Transl.)*
[c] — *Chem. Phys. Rep. (Engl. Transl.)*
[d] — *Bull. Moscow Univ., Chem. (Engl. Transl.)*
[e] — *Dokl. Phys. Chem. (Engl. Transl.)*
[f] — *Russ. J. Inorg. Chem. (Engl. Transl.)*
[g] — *Russ. J. Organomet. (Engl. Transl.)*
[h] — *J. Struct. Chem. (Engl. Transl.)*
[i] — *Russ. J. Phys. Chem. (Engl. Transl.)*
[j] — *Russ. Chem. Bull., Int. Ed. (Engl. Transl.)*